TAMPERE UNIVERSITY OF TECHNOLOGY

TATIANA EFIMUSHKINA

REVERSIBLE DATA HIDING IN DIGITAL IMAGES

Master's thesis

Examiners: Professor Karen Egiazarian
Professor Yevgeni Koucheryavy
Professor Moncef Gabbouj
Examiners and topic approved by the Faculty Council of the Faculty of Computing and Electrical Engineering on 9 January 2013.

Preface

This thesis concludes a long-term research on reversible data hiding leaded in TUT under supervision of Professor Karen Egiazarian, which was started in summer 2011. Research topic revealed in the thesis refers to my Master's Minor studies; therefore, during the last year, a lot of experience and knowledge was initially gained before observable results have been obtained. This thesis describes in detail the achieved results, which were published in several conference papers, and comprises a self-sufficient study on the state-of-the-art data hiding algorithms.

I wish to express my gratitude to Professor Karen Egiazarian for giving me the chance to pursue the studies for my Master's thesis in Finland and for his highly professional guidance.

I am very grateful to Professor Yevgeni Koucheryavy for his natural ability to involve students, and particularly me, into research work that resulted in successful cooperation and several joint publications in the field of communications engineering.

Moreover, I would like to thank Professor Moncef Gabbouj for his prompt important comments on the structure of the work and language, and for valuable advices.

I also wish to thank my family and my boyfriend who managed to create an appreciating environment that helped me to overcome the hardest moments.

27.11.2012
TATIANA EFIMUSHKINA

Abstract

TAMPERE UNIVERSITY OF TECHNOLOGY

Master's Degree Programme in Information Technology

EFIMUSHKINA, TATIANA: "REVERSIBLE DATA HIDING IN DIGITAL IMAGES"

Master of Science Thesis, 51 pages, January, 2013

Major subject: Communications Engineering

Minor subject: Signal Processing

Examiners: Professor Karen Egiazarian, Professor Yevgeni Koucheryavy, Professor Moncef Gabbouj.

Keywords: Location map free, reversible data hiding, difference expansion, histogram shifting, Galois field, MED, GAP, JPEG.

Nowadays the role of data hiding has become more eminent. The data safety on the Internet is known to be a challenge due to frequent hacker attacks and data tampering during transmission. In addition to encryption schemes, data hiding has an important role in secret message transmission, authentication, and copyright protection.

This thesis presents in-depth state-of-the-art data hiding schemes evaluation, and based on the conducted analysis describes the proposed method, which seek the maximum improvement. We utilize a causal predictor and a local activity indicator with two embedding possibilities based on difference expansion and histogram shifting. Moreover, the secret data from Galois field $GF(q), q \leq 2$ in order to embed more than one bit per pixel in a single run of the algorithm is considered. We extend our data hiding technique to the transform domain complaint with JPEG coding. In the experimental part, the proposed method is compared with state-of-the-art reversible data hiding schemes on a vast set of test images, where our approach produces better embedding capacity versus image quality performance. We conclude that proposed scheme achieves efficiency in terms of redundancy, which is decreased due to the derived conditions for location map free data embedding, invariability to the choice of predictor, and high payload capacity of more than 1 bit per pixel in a single run of the algorithm.

Contents

Abbreviations and symbols

- AC (Alternating Current) – a DCT coefficient with non-zero frequencies that represents the change of color in a block of interest in terms of image processing.
- CALIC (Context-based, Adaptive, Lossless Image Codec) – a lossless codec, that achieves high compression ratio of continuous-tone images.
- DC (Direct Current) – a DCT coefficient with zero frequency in both dimensions that represents the average energy of the signal.
- DCT (Discrete Cosine Transform) – a Fourier related transform using real numbers used in lossy compression of audio and images.
- DE (Difference Expansion) – a lossless data-hiding algorithm, which divides the image into pairs of pixels, and then embeds one bit into the difference of the pixels of each pair from those pairs that are not expected to cause an over/underflow. The location map that indicates the modified pairs is included into the payload.
- GAP (Gradient Adjusted Prediction) – an efficient predictor, which tries to use the context gradient information to predict the intensity of the current pixel, which is a part of CALIC algorithm.
- HS (Histogram Shifting) – a lossless data-hiding algorithm, which uses pairs of zero points and peak points of the histogram, and shifts the part of the histogram between the peak and min points in order to obtain space for secret message embedding. Location map is necessary to prevent over/underflow.
- IWT (Integer Wavelet Transform) – a basic modification of linear transforms, where each filter output is rounded to the nearest integer. When applying the integer wavelet Haar transform to the input image, four bands of integer wavelet approximation coefficients LL, and details coefficients HL, LH and HH (in horizontal, vertical and diagonal direction, respectively) are obtained.
- JPEG (Joint Photographic Experts Group) – a standard that specifies a commonly used method of lossy compression for digital images.
- LAI (Local Activity Indicator) – a measure of some statistical dispersion (e.g. a maximum absolute deviation), which is used in data hiding to control embedding of secret data.
- LM (Location Map) – an image of the same size as the original one, which marks the positions of the pixels of interest. Usually the rest of the pixels are zeros.
- LSB (Least Significant Bit) – a bit position in a binary integer giving the units value.

- MED (Median Edge Detection) – a primitive predictor, which allows to detect horizontal or vertical edges by examining the neighboring pixels of the current pixel. It is utilized in JPEG-LS lossless compression standard.
- MSE (Mean Squared Error) – one of the way to measure the difference between the estimator and the quantity to be estimated, or in terms of data-hiding between the cover and stego images.
- PE (Prediction Expansion) – a reversible watermarking technique, which expands the difference between the target pixel and its estimate called predictor.
- PSNR (Peak Signal-to-Noise Ratio) – a measure of quality of a watermarked image, which is measured in decibels [dB].
- RGB (Red Green Blue) – a color space, which is based on the color model, in which red, green, and blue are added together in various ways to reproduce a broad array of colors.
- SSIM (Structural Similarity) – a method for measuring similarity between two images that is designed to improve PSNR and MSE methods, which have proved to be inconsistent with human eye perception.
- WSP (Weighted Simplified Predictor) – a predictor that estimates the target pixel by considering its closest neighboring pixels and taking the weighted average of them. It was introduced in [3] and provides very efficient prediction in terms of computational costs.

Table 1: Symbols and Notation

Variable	Description
$\mathbf{I} = [I_{i,j}]$	The cover $M \times N$ image, $i = \overline{0, M-1}, j = \overline{0, N-1}$
$GF(q)$	Galois field of order q
w_s	Secret message with elements from Galois field, $w_s \in GF(q)$
$\widehat{I_{i,j}}$	The predicted pixel at the spatial location (i, j)
$E_{i,j}$	The prediction error at the position (i, j)
$d_{i,j}$	Local activity indicator computed over a region of a pixel at the position (i, j)
$T^{\mathrm{DE}}_{low}, T^{\mathrm{DE}}_{high}$	The two thresholds that control DE embedding of the secret data
$T^{\mathrm{HS}}_{low}, T^{\mathrm{HS}}_{high}$	The two thresholds that control HS embedding of the secret data
$\tilde{I}_{i,j}$	The watermarked pixel at the position (i, j)
$E^{new}_{i,j}$	New prediction error, which is found at the reconstruction stage
Q	User-specified parameter that bounds the prediction error
K	Number of the image levels
AC_k	Separate plane, which consists of kth AC coefficients from every 8×8 block after DCT is performed
h	User-specified parameter that allows to gain flexibility of the HS scheme
Q_f	Quality factor of the quantization operation
μ_+, $\mu_\times$, μ_C, μ_S	Number of additions, multiplications, comparisons and shift operations, respectively

List of Tables

List of Figures

1 Introduction

Nowadays with the growth in the information technology, there has opened new opportunities in scientific and commercial applications. However, this progress has caused a lot of serious problems including hacking, duplications and malevolent usage of digital information. Steganography which refers to the secret communication tries to address these growing concerns. A secret message is embedded into a host or cover signal (original audio, image or video data) by slightly modifying its content that results in a watermarked or stego signal as shown in Figure 1. The reverse operation is called extraction. Note that steganographic applications have no value for the host signal, which plays the role of a decoy to conceal the very presence of communication. In that case, non-reversible schemes are used, in which only the secret message is extracted. However, there is a number of other applications, which require both the cover image and the secret message at the output and are based on computationally heavy reversible or lossless data hiding techniques. This group of applications aka digital watermarking related closely to the cover signal. The secret message comprises the additional data about the signal, which increases its practical value, however, introduces some amount of distortion. Note that some applications cannot sustain any distortion, e.g. medical imagery, where every bit of information is important.

Figure 1: Data embedding terms

1.1 Data hiding main terms and notions

Among the lossless techniques of data embedding there are two common domains of operation: spatial and frequency. Spatial techniques are characterized by the embedding of messages into the least significant bits (LSBs) of image pixels, while in frequency methods the message is embedded after a certain transform is performed by modifying frequency coefficients of the cover image. Transform embedding methods are known to

be in general more robust than the spatial embedding schemes, which are susceptible to image-processing types of attacks. However, spatial data hiding techniques provide in general higher capacity, which is defined to be a number of bits that can be embedded into the signal. It should be noted that capacity is closely connected to the quality measure known as perceptibility. Perceptibility or fidelity shows whether the source cover is distorted by embedding information to a visually unacceptable level.

In order to obtain a deeper insight of the data hiding process in images, it is necessary to summarize the definitions of the following terms and notions:

- reversibility: ability to extract both the original image and the watermark;
- perceptibility: perceptual similarity between the original and the stego images;
- payload: number of encoded bits of a watermark without including the redundant information;
- robustness: ability to detect the watermark after the common signal processing operations;
- capacity: number of bits that can be embedded into the signal.

The performance of the data hiding methods can be measured by the payload capacity limit, visual quality and complexity [1], where the visual quality is the quality of the stego image after the embedding operation is done, and complexity is a number of mathematical operations, which describes the algorithm.

Another classification criteria of data hiding schemes is the actual technique of data embedding, among which the most common are: compression, histogram shifting (HS) and difference expansion (DE). This thesis will provide thorough explanations in the next chapters of DE and HS techniques which achieve high embedding capacity preserving the imperceptibility of the signal.

All in all, embedding of secret message inevitably will cause some distortion of the cover image. It is highly desirable that this distortion be as small as possible while meeting other requirements, such as sufficient capacity and robustness. In previous work [2], [3], we developed DE and HS schemes, respectively, which showed excellent payload versus quality performance. This thesis concludes the performed research, and acts as a complete reference of the results obtained so far. We combine both schemes into one general data embedding algorithm and extend it to the joint photographic experts group (JPEG) format images. Utilization of the secret message with the elements from Galois field allows to hide almost 1 bit per pixel in case a binary message is considered without high degradation of the image. Note that the proposed generalized algorithm sustains the reversibility concept and can be applied to both spatial or frequency discrete cosine transform (DCT)-based domains of operation. We compare the proposed technique with [4] and [5], where the advantage in terms of the payload versus image quality is shown.

1.2 Structure of the thesis

The thesis is organized as follows. The theoretical background in section 2 provides insight into the common data hiding DE [1] and HS [6] schemes and algorithms which present the prototype and base for further developed reversible data embedding schemes. Moreover, two state-of-the-art techniques [4] and [5], which are used for comparison with the proposed algorithm are discussed in detail. Then the major constraints of the general DE and HS approaches and our contributions to improve their performance are presented.

The proposed generalized q-ary schemes with the formulated DE and HS embeddings are developed in Section 3, where the mixed algorithm with DE and HS embeddings is also described. Section 4 reveals the extension of the proposed data embedding procedure to JPEG images. It specifies the challenges and main steps of embedding the data into the frequency domain.

The experimental results are illustrated in Section 5. Finally, conclusions are drawn.

2 Theoretical background

Based on the discussion in the introduction section, let us have a look at data hiding schemes that other researchers have proposed in literature. As it was mentioned above among the reversible techniques of data embedding the most common are: compression, histogram shifting and difference expansion. However, let us start examining data-hiding methods with the first published reversible additive watermarking technique investigated by Honsinger et al. [7], who proposed to embed the watermark w by using modulo-256 addition. Then the watermarked image $\tilde{\mathbf{I}}$ can be found $\tilde{\mathbf{I}} = (\mathbf{I} + w) \mod 256$, where $\mathbf{I}$ is the original image. At the extraction stage the concept of reversibility is preserved by subtracting the secret message from the watermarked image. However, if we select the 8-bit original image that is frequently considered for data-hiding, which comprises gray values from 0 to 255, the problem of under/overflow is avoided. Here, under/overflow corresponds to the scenario when pixel values exceed minimum and maximum possible limits. So in the particular case, a pixel has a value less than 0 or greater than 255, respectively. Hence, though reversibility and under/overflow issues are addressed, the greatest drawback of the scheme is the salt and pepper noise caused from the overflow avoidance. Another method proposed by Macq [8] is based on the usage of multiresolution image coefficients for embedding the secret message by applying the sum modulo operation in the transform domain. However, the problem of salt and pepper noise is not solved.

Compression based algorithms reversibly embed data by means of lossless compression and can be utilized both in spatial and frequency domains. Fridrich et al. [9] compressed the LSB plane to obtain extra space for embedding the secret data. The compressed original image features as well as their location information also known as location map (LM) are embedded along with the payload. Celik et al. [10, 11] extended Fridrich's scheme by proposing the generalized-LSB scheme. In the embedding stage, the original signal is quantized and the residual is obtained. In order to obtain free space for hiding the secret message, a lossless compression algorithm for images (CALIC) is applied to the residuals. Residual information represents redundant information that should be added to the payload to provide perfect reconstruction of both the host image and secret data.

2.1 Difference expansion approach

Difference expansion is a specific case of the expansion embedding technique, which utilize the decorrelating process to find the elements with small magnitudes. The embedding is done by expanding those elements to obtain vacant positions, where the bits will be inserted. Note that the expansion of the elements may cause stego image's distortion, therefore, in order not to degrade the quality, the magnitudes of the obtained elements are to be very small. DE can be referred to the expansion embedding technique with the pixel differences representing the elements with small magnitudes. Pixel differences im-

ply high redundancies of the neighboring pixel values in original images and, therefore, are the ones to be used for embedding.

2.1.1 Tian's scheme

Tian was the first one who introduced in [1] the difference expansion algorithm, that has been revolutionary in the reversible watermarking scenario. The steps of the algorithm based on integer Haar wavelet transform are presented below:

1. Divide an image into pairs, compute the average l (low-frequency) and difference h (high frequency) components between neighboring two pixels. Therefore, forward transform for an 8 bits grayscale pair (x,y) is defined:

$$l = \lfloor \frac{x+y}{2} \rfloor, h = x - y. \tag{1}$$

Then the inverse transform of (1) is obtained

$$x = l + \lfloor \frac{h+1}{2} \rfloor, y = l - \lfloor \frac{h}{2} \rfloor. \tag{2}$$

In order to prevent under/overflow, the following conditions have to be fulfilled:

$$0 \leq l + \lfloor \frac{h+1}{2} \rfloor \leq 255, 0 \leq l - \lfloor \frac{h}{2} \rfloor \leq 255. \tag{3}$$

The defined conditions are equivalent to:

$$\begin{cases} h \leq 2l+1, & \text{if } 0 \leq l \leq 127, \\ h \leq 2(255-l), & \text{if } 128 \leq l \leq 255. \end{cases} \tag{4}$$

2. Divide the differences into two sets: expandable (5) and changeable (6) depending on which condition is satisfied:

$$| 2h + w | \leq \min(2(255-l), 2l+1), \tag{5}$$

$$| 2\lfloor \frac{h}{2} \rfloor + w | \leq \min(2(255-l), 2l+1), \tag{6}$$

where w is the secret message to be embedded.

3. Data embedding is done by appending the bit to the LSB of the pixel difference from the expandable set, and by the replacing the LSB of the pixel difference from changeable set with the information bit.

In order to get the full view of the algorithm it is necessary to provide the detailed description of various sets of difference values. Tian in [1] created four disjoint sets of difference values known as EZ, EN, CN, and NC, which contain all:

- EZ: expandable $h = 0$ and expandable $h = -1$ differences;
- EN: expandable $h \notin$EZ;
- CN: changeable $h \notin$(EZ $\bigcup$ EN);
- NC: nonchangeable h.

The embedding of bit b on difference values from various sets is shown in Table 2.

4. Expandable and not expandable pairs are mixed, so to enable lossless reconstruction their positions are saved in a location map, which is losslessly compressed in order to release room for useful payload. During data embedding process, all changeable difference values are modified. In order to guarantee an exact recovery of the host image the original values of the modified LSBs have to be also embedded. After all the payload and redundant data have been embedded in the image the reverse transform is applied.

5. Reconstruction is done in a similar way, at the result of which the original image and the watermark are obtained. So at the receiver side at first the integer transform is computed, then all changeable differences are selected and the LSBs are collected. Then location map is decompressed, so by scanning it, expandable and changeable differences are identified. The secret message and the original LSBs are extracted afterwards. The major drawback of the scheme is that the maximum theoretical capacity, without taking into account the size of the location map, is equal to the half of size of the image.

Let us consider a simple example of the difference expansion presented in [1]. We assume that there are two pixel values $x = 206, y = 201$, and one bit is to be embedded reversibly $b = 1$. At the first stage integer average and difference values are computed $l = \lfloor \frac{206+201}{2} \rfloor = 203$ and $h = 206 - 201 = 5$. When performing the embedding operation we get $h' = 2h + b = 11$. Finally new pixel values are computed $x' = 203 + \lfloor \frac{11+1}{2} \rfloor = 209, y' = 203 - \lfloor \frac{11}{2} \rfloor = 198$. At the extraction phase again the integer average and difference are found from the embedded pair $(x', y') = (209, 198)$. So $l' = \lfloor \frac{209+198}{2} \rfloor = 203, h' = 209 - 198 = 11$. The binary representation of $h' = 11 = 1011_2$. After extracting the LSB we get $b = 1$, and $h = \lfloor \frac{h'}{2} \rfloor = 5$. Now using the integer average value l' and restored difference value h, the exactly original pair (x, y) is obtained.

The major constraint of the following scheme comprises the capacity limitation, which stems from the necessity to embed the compressed LM along with the useful payload. Moreover, pairing the pixels do not effectively exploit the correlation inherent in a neighborhood, particularly if multiple or recursive embedding is done with various directions of

Table 2: Embedding on difference values

Original Set	Original Value	Location Map Value	Watermarked value
EZ or selected EN	h	1	$2h + b$
CN or not selected EN	h	0	$2\lfloor \frac{h}{2} \rfloor + b$
NC	h	0	h

pixel pairing. Alattar [12, 13] extended Tian's algorithm by operating on vectors instead of pairs of pixel values to increase the data hiding capacity and the computation efficiency of the algorithm. This approach allows to embed several bits in every vector in a single pass through the image.

Another strategy introduced by Thodi et al. [14] implies decorrelation of the image using a predictor, which can better exploit the correlation inherent in the neighborhood of the pixel and is called prediction error expansion (PE). It is one of the most popular technique of reversible watermarking. Instead of expanding the difference between two adjacent pixels as was done in Tian's method, PE technique expands the difference between a target pixel and its estimate. So the main advantages of the approach is that the predictor generates the elements with much smaller magnitudes than the difference operator. In his first version Thodi performed the prediction with the help of the median edge detection (MED) used in JPEG-LS compression standard [14], while in the second version [15], a threshold was selected for prediction error magnitudes. So far, several versions of PE reversible data hiding methods have been proposed [16]-[18]. Moreover, Hu et al. [19] proposed an embedding algorithm in the S-transform, which utilizes the horizontal as well as vertical image differences for data hiding. Luo et. al. [20] introduced an improvement of the difference expansion scheme by considering original image pixels and the same pixels estimated by interpolation.

2.1.2 Coltuc's scheme

Different researchers [16]-[19] aimed at reducing various factors in PE schemes, such as auxiliary data, prediction error or embedding distortion. Coltuc in [4] focuses on reducing the embedding distortion for PE reversible data hiding. He proposed a modified data embedding for prediction error expansion where the prediction is performed into the current pixel and the prediction content. Moreover, the optimization of the embedding for various predictors is analyzed.

Before describing the optimized embedding principle of the PE watermarking as in [4], it is necessary to remind the PE embedding equation, which enables to find the watermarked pixel X provided that there is no under/overflow:

$$X = \widehat{x} + 2(x - \widehat{x}) + w, \tag{7}$$

where x and $\widehat{x}$ are the target pixel and its estimate computed on a neighborhood V^x, while w is a bit to be embedded. In other words, $X = x + (x - \widehat{x}) + w$ and the prediction error $p = x - \widehat{x}$ and the secret bit w are added to the grayscale value of the pixel. At the extraction stage, first the secret message is extracted:

$$w = (X - \widehat{x}) - 2\lfloor \frac{X - \widehat{x}}{2} \rfloor. \tag{8}$$

As soon as the secret data is restored, the original pixel can be found:

$$x = \frac{(X + \widehat{x} - w)}{2}. \tag{9}$$

It can be seen that the error is expanded with $p_w = x - \widehat{x} + w$, which is fully embedded into the target pixel. Instead Coltuc in [4] introduced an approach when the embedding of p_w is conducted not only to the target pixel but also to its content. The modification of the content is done using by the function ϕ in the following way:

$$V_\delta^x = \phi(V^x, \delta), \tag{10}$$

where δ represents a certain fraction of p_w with α fixed, $0 \leq \alpha < 1$:

$$\delta = \lfloor \alpha p_w + 1/2 \rfloor. \tag{11}$$

Thus, the new value of x becomes:

$$X_\delta = X - \widehat{x} + \widehat{x}_\delta, \tag{12}$$

where $\widehat{x}_\delta$ is the estimate of x on the modified neighborhood V_δ^x. The extraction operation is conducted similarly to PE case. Note that the described above modified scheme depends on function ϕ and δ, which define and control the procedure, respectively. The function ϕ splits the data to be embedded between the target pixel and its context, while δ controls the amount of data to be embedded. The scheme is a prediction based state-of-the-art watermarking technique, which operates efficiently for any chosen predictor. However, the modification of the neighborhood of the current pixel may decrease the correlation between pixels, and, consequently, degrade the performance of the prediction scheme. Therefore, the global optimization is required by varying the values of δ.

For better understanding, let us consider the improved embedding for MED predictor, which is known to show an excellent performance in JPEG-LS standard [19] and is presented below:

$$\widehat{x}_{i,j} = \begin{cases} \max(a,b), & \text{if } c \leq \min(a,b), \\ \min(a,b), & \text{if } c \geq \max(a,b), \\ a+b-c, & \text{otherwise}, \end{cases} \tag{13}$$

where $a = x_{i,j-1}$, $b = x_{i-1,j}$, and $c = x_{i-1,j-1}$.

Note that in order to protect against under/overflow control and preserve the reversibility property, the location map which indicates the embeddable positions has to be appended to the payload. Therefore, the function ϕ is defined:

$$\phi(a,b,c,\delta) = (a_\delta, b_\delta, c_\delta) = (a-\delta, b-\delta, c-\delta). \tag{14}$$

For the modified content the prediction is $\widehat{x}_\delta = \widehat{x} - \delta$, and the watermarked pixel can be obtained:

$$X_\delta = x + p_w - \delta. \tag{15}$$

Similarly, at the detection stage, the secret message w is obtained as the LSB of $X_\delta - \widehat{x}_\delta$, and the original pixel and its content can be restored:

$$x = X_\delta - p_w + \delta, a = a_\delta + \delta, b = b_\delta + \delta, c = c_\delta + \delta. \tag{16}$$

As it was said above the optimization procedure is required in order to minimize the square error E^2 introduced by watermarking p_w^2. Therefore:

$$E^2 = (X_\delta - x)^2 + (a_\delta - a)^2 + (b_\delta - b)^2 + (c_\delta - c)^2 = p_w^2 - 2\delta p_w + 4\delta^2. \tag{17}$$

By solving the equation $\frac{\partial E}{\partial \delta} = 0$, the value $\delta_0 = p_w/4$ gives the minimum value $E^2_{min} = 3/4p_w^2$. In case, $\delta_0 = 0$ corresponds to the classical PE technique. Note that the described scheme is a state-of-the-art approach that is able to achieve a high increase in quality of the stego image.

2.2 Histogram shifting approach

The histogram shifting approach implies lossless embedding of the secret data by shifting the bins of the image's histogram. Image histogram represents a plot with a number of pixels in vertical direction for each grayscale value of the image in horizontal direction.

2.2.1 Ni's scheme

Ni was the first to introduce the realization of the following scheme in [6], the general steps of which are presented below. The embedding procedure can be visualized in Figure 2.

1. Generate image histogram $H(x)$.

2. Find the maximum value $h(a)$ (peak point) and the minimum value $h(b)$ (min point) of the constructed histogram $H(x)$.

3. Store the image pixel positions that correspond to the value of the min point of a histogram in a LM and zero the min point histogram bin $h(b) = 0$.

4. Without loss of generality, assume that $a < b$. Move the histogram values that are situated between the peak and min points to the right by 1 unit, which implies increasing the corresponding pixel values by one.

5. Scan the image and on encountering peak point, embed "1", i.e. enlarge the pixel value by one. If the secret bit is "0", there is no need to change the pixel value.

1. Find the **peak** point and the **min** point of the image histogram *H(x).*	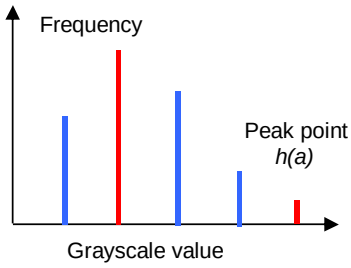
2. Store the image pixel positions of the **min** point in a location map and zero the **min** point histogram bin *h(b)*=0.	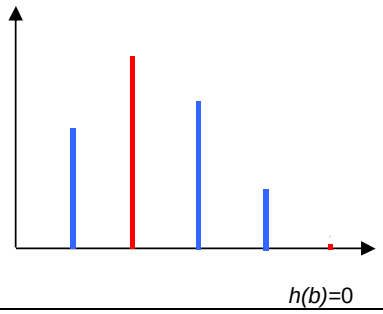
3. Move the histogram values that are situated between the **peak** and **min** points to the right by 1 unit.	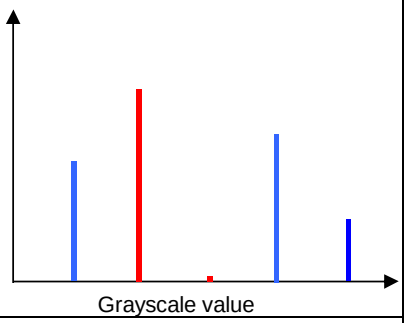
4. Enlarge the pixel value by one if the secret bit is 1, if the bit is 0 there is no need to change the pixel value.	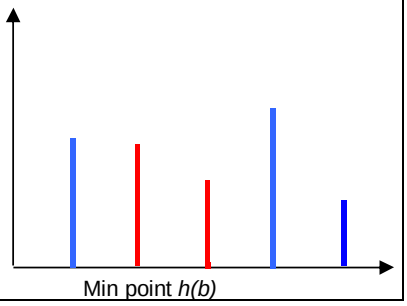

Figure 2: Data embedding algorithm introduced in [6]

It is worth noticing that the peak point of the histogram defines the capacity of the scheme. Therefore, actual data embedding capacity, C, is calculated as follows:

$$C = h(a) - O, \tag{18}$$

where O is the amount of data used to represent the overhead information. In case the required payload is greater than the actual capacity, then more pairs of maximum point and minimum point are necessary.

At the extraction stage the following algorithm should be followed in order to reconstruct reversibly the image and the secret message:

1. Scan the watermarked image. If a pixel with grayscale value $a+1$ is encountered, a bit 1 is extracted. In case value a is considered, a bit 0 is extracted.

2. Scan the image for the second time and subtract by 1 the pixel values, whose grayscale values are in the interval $(a,b]$.

3. Set the pixel grayscale value as b recorded in location map.

Therefore, the original pixel can be recovered. Among the advantages of the introduced scheme are:

1. Simplicity.

2. Distortions are almost invisible.

3. High capacity.

It is obvious that this capacity is connected to the occurrence of pixel with the same frequency of the peak value. Moreover, there can be a scenario when images do not have zero points. So to improve the capacity and to make the algorithm work also if there are no zero points, the general form is to utilize multiple pairs of minimum and maximum points (that are transmitted as overhead information). The drawbacks of this method are:

1. The distribution of minimum points can influence the embedding procedure. For example, if two minimum points are in the same side of the maximum point, then only one pair of maximum and minimum points can be selected.

2. The maximum and minimum points represent redundant information.

3. Multiple image scanning is time consuming.

In [21] Yang et al. adopted the same method of Ni to find optimal multiple pairs of maximum and minimum points. The introduced method examined the waveform of the histogram, and it selected the maximum point from the various zones of the histogram (crests and troughs). In [22] Hwang et al. extended the method of Ni by applying the algorithm of searching two minimum points and one peak point of a histogram. Chang et al. in [23] proposed a similar method to [6] operating on peak values, but introduced the usage of the absolute values of horizontal differences between two adjacent pixels. Other researchers [24]-[29] found a way to increase the embedding capacity by exploiting the prediction error histogram, which is found by computing the difference between the original pixel and the predicted value of the image. Keeping in mind that the peak height of the prediction error histogram is usually higher than that of the image histogram for most images, a higher payload can be achieved. The histogram of the original 8-bit "House" image and prediction error histogram, obtained by utilizing the gradient adjusted prediction (GAP) [29], are shown in Figure 3. Note that an accurate prediction contributes significantly to get a higher peak value of the histogram.

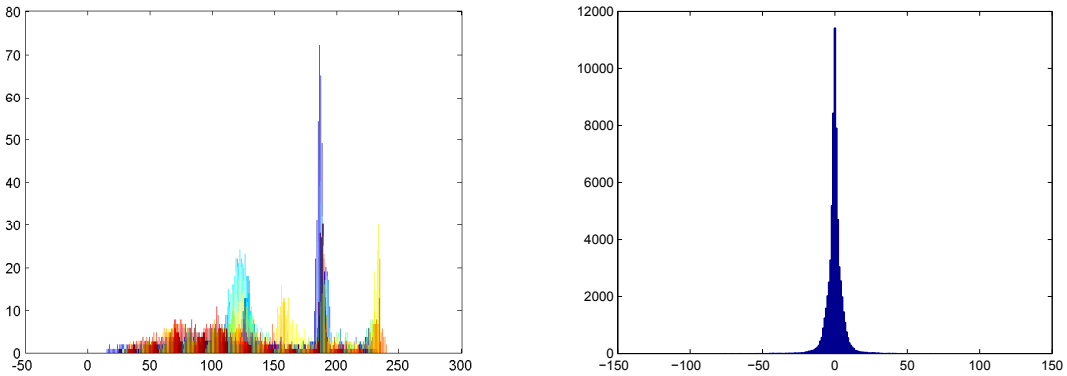

Figure 3: Histogram and prediction error histogram of ”House” image from left to right, respectively

2.2.2 Xuan's scheme

It is well-known that the histogram distribution varies dramatically from one image to another, therefore in order to achieve high payload without bringing significant degradation to an image, some additional methods are required. Xuan et al. [5] proposed a different histogram shifting approach working on the coefficients of the high frequency bands obtained by applying the integer wavelet transform (IWT) to the cover image. In Figure 4 the original Barbara image and its counterpart after IWT transform is shown. Note that when applying the integer wavelet Haar transform to the input image, four bands of integer wavelet coefficients that correspond to low frequency approximation coefficients LL, and high frequency details coefficients HL, LH and HH (in horizontal, vertical and diagonal direction, respectively) are obtained.

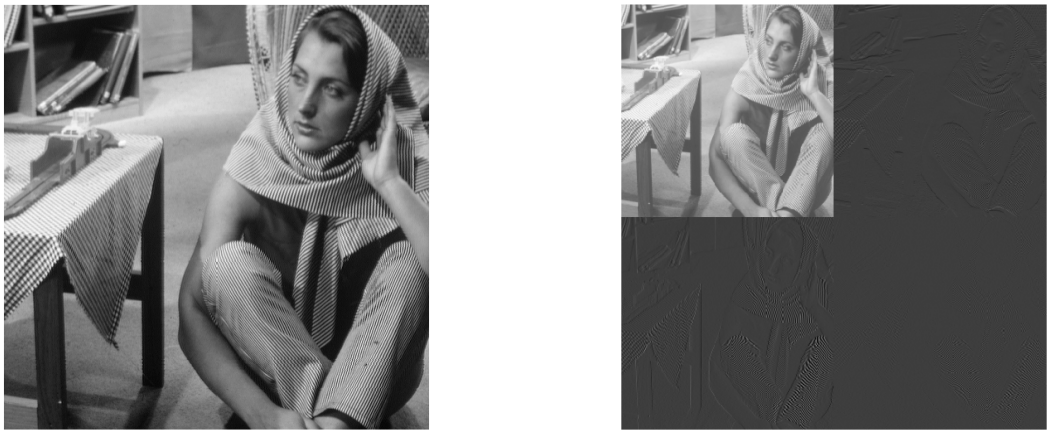

Figure 4: Original Barbara image and Barbara after Haar transform from left to right, respectively

Since the wavelet coefficients of high frequency subbands have Laplacian-like distri-

bution with high peak in the histogram around zero, it was proposed to consider histogram shifting scheme after IWT was applied to the original image. Refer to the Figure 5, where the principle of data embedding using histogram shifting is demonstrated. In Figure 5 there are two histograms: the first one, which corresponds to the histogram after IWT is applied to the original image, and the second one, which contains the zero point that is found after the threshold is chosen. The part of the histogram with values larger than the threshold Z are shifted to the right by one unit, while the part of the histogram with values less than Z remains unchanged.

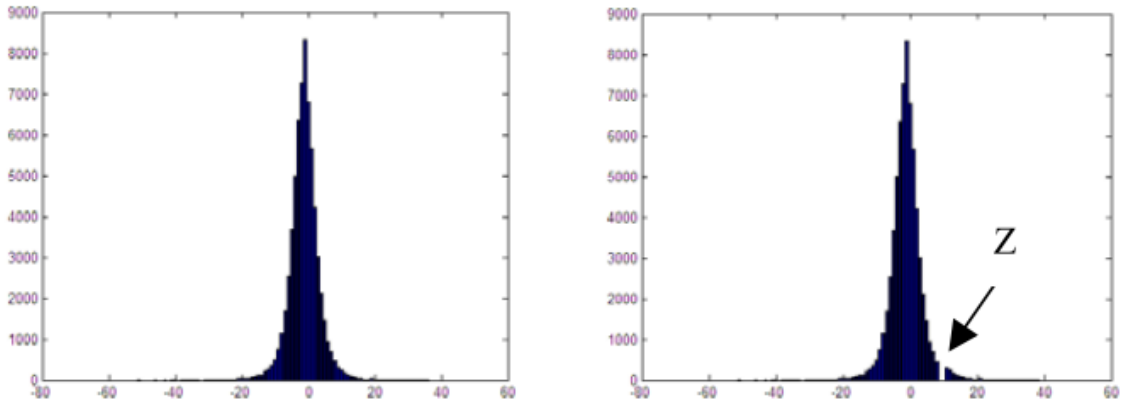

Figure 5: Histogram of the image after IWT and histogram with the created zero point from left to right, respectively [5]

The data-embedding is done in the following way: when scanning the high-frequency subband and encountering the value "Z", if the secret bit is equal to "1", the watermarked coefficient will be "$Z+1$". However, if the to-be-embedded bit is "0", the coefficient remains the same "Z". The extraction is done in the reverse manner: if the scanned value of the stego image is "$Z+1$", then it is supposed that the bit "1" is hidden, and the value is reduced to "Z". When "Z" is encountered, bit "0" is found and extracted. After all data have been extracted, the part of the histogram equal to or larger than "$Z+2$" needs to be shifted towards the left side by one unit. The histogram of IWT high frequency subband obeys Laplacian-like distribution, therefore, the procedure can be conducted in both sides of the histogram alternatively until all secret bits are embedded. The more detailed explanation of the embedding and extraction procedures are presented in Figures 6, 7 and in step-by-step clarifications below.

Let us suppose that there are M bits which are supposed to be embedded into the high frequency subband after IWT was performed. The data is embedded in the following way:

1. The threshold is specified $T > 0$ with the assumption that the number of the high frequency wavelet coefficients in $[-T,T]$ exceeds M. Then, the parameter *Peak* is set to equal T.

2. A zero point is obtained by moving the histogram to the right by one unit at the

value of $Peak + 1$. The next procedure is to hide the secret data as described above.

3. In case not all the payload was embedded, let $Peak = -Peak$ and obtain a zero point at the value $-Peak - 1$. Perform data hiding.

4. In case all the secret bits are embedded, stop the procedure and record the *Peak* value as stop value, S, otherwise $Peak = -Peak - 1$, and the embedding operation is continued by going back to step 2.

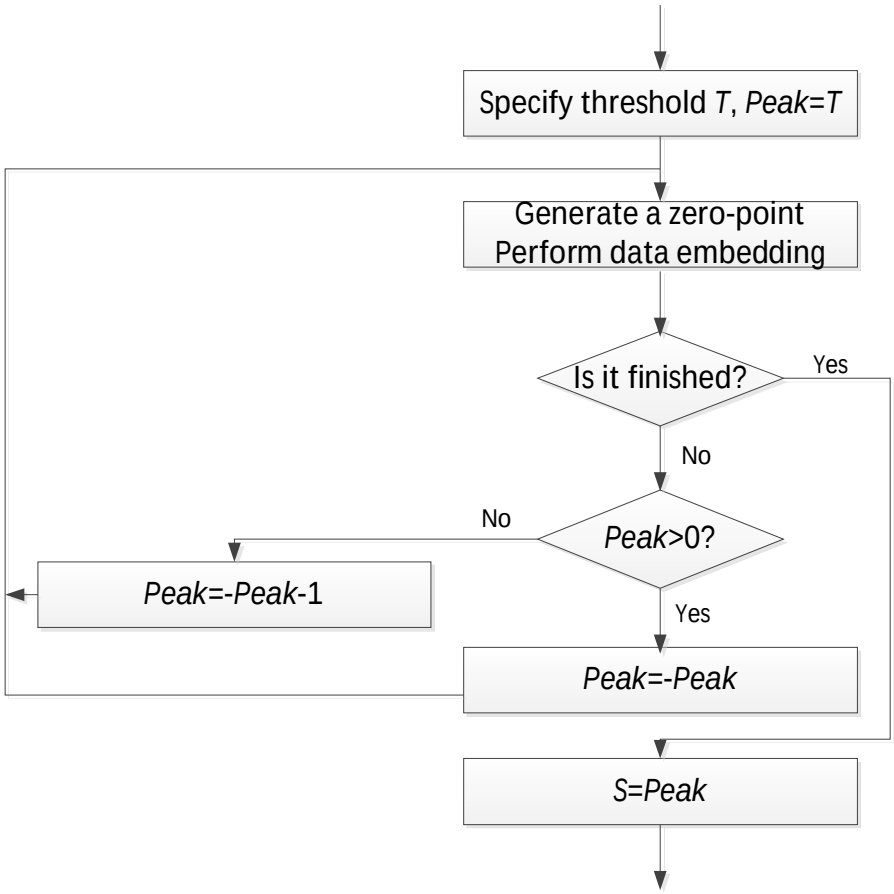

Figure 6: Data hiding algorithm introduced in [5]

At the extraction stage it is assumed that the values of the stop parameter S and the threshold T are known. The data extraction algorithm is shown in Figure 7 and comprises the following steps:

1. Set *Peak* to equal to the stop value S.

2. Extract all the secret data until $Peak + 1$ is a zero point. Then move the part of the histogram, which is greater than $Peak + 1$ to the left by one unit to cover the zero point.

3. In case the extracted data is less than M, then set $Peak = -Peak - 1$ and continue the extraction process until it becomes the zero point in $Peak - 1$. Again move the part of the histogram, which is less than $Peak - 1$ to the right by one unit to cover the zero point.

4. Stop if the hidden message if fully extracted. Otherwise, set $Peak = -Peak$ and continue the extraction process by returning to step 2.

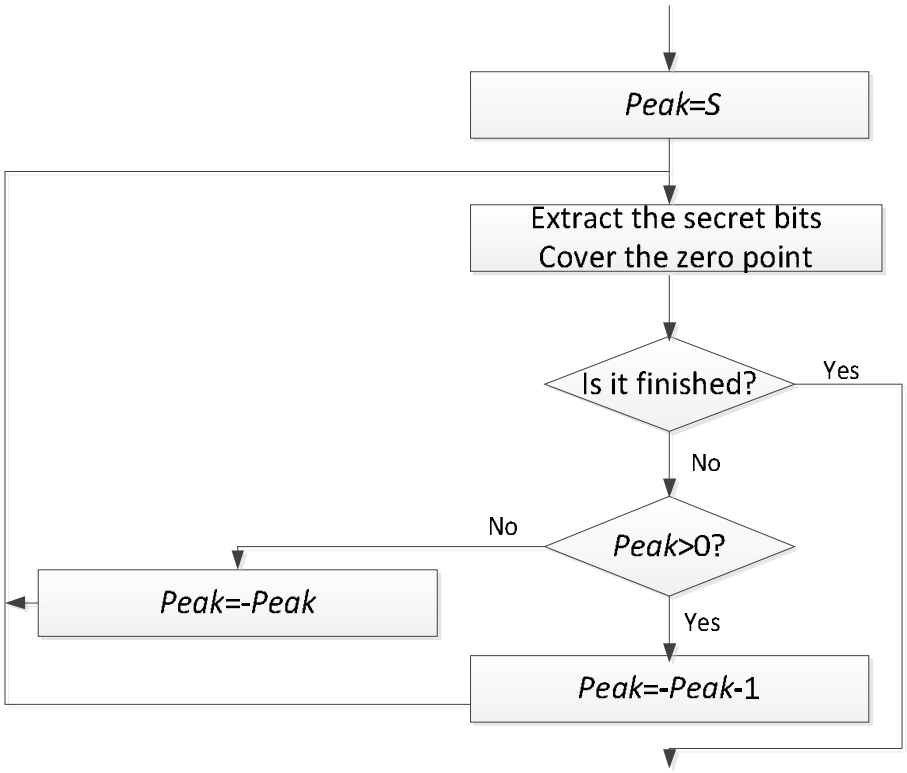

Figure 7: Data extraction algorithm introduced in [5]

After all the bits of the secret message has been extracted, the inverse integer wavelet transform is applied and the original image is restored. Note that embedding in the frequency domain can cause under/overflow, which means that after inverse wavelet transform the grayscale values of some pixels in the watermarked image may exceed the lower or upper bound. Therefore, some control operation is necessary, which is applied before the watermarking procedure and consists of narrowing the histogram of the original image from both sides. The overhead information is constructed by recording the shift of each modified pixel, and it is embedded with the payload to allow lossless reconstruction. In the experimental part, Xuan showed that the scheme's performance achieves higher capacity versus quality results comparing to a number of data hiding techniques [6, 21].

2.3 DCT-based schemes

Most of the schemes mentioned above operate in the spatial domain with the secret message being embedded directly into the pixel values. These schemes are characterized

by the high payload versus stego image quality performance; however, they lack robustness against various image-processing types of attacks. Transform-based techniques embed the data into the frequency coefficients of the signal, after a certain transform has been applied to the original signal, such as DCT. Note that transform-based data hiding techniques achieve a higher robustness but suffer from a small amount of payload being embedded without introducing a significant distortion. JPEG is a widely used compression standard for transmission and storage of digital images and, therefore, is commonly used by data-hiding techniques. Chang et al. [30] embedded the secret data in the middle-frequency part of the quantized DCT coefficients. In [31] Fridrich et al. designed a simple scheme for three most common image format paradigms: raw, uncompressed (BMP), transform (JPEG) and palette losslessly compressed formats (GIF, PNG), where the least significant bit plane of some selected JPEG coefficients is losslessly compressed in order to obtain room for data embedding. Xuan et al. in [32] proposed the reversible data hiding scheme for JPEG images based on histogram pairs aiming at improving the scalability. The produced histogram pairs contain an original position and an expansion position, which are utilized when the to-be-embedded bits are 0 and 1, respectively. Sakai et al. [33] has improved Xuan's scheme by proposing an adaptive reversible embedding scheme, where the bits are hidden only into the smooth areas of the image. To single out the smooth areas, variances of the DC components among neighboring blocks are computed. However, the algorithm does not work well in noisy images, where the correlation among DC components is relatively small, which results in high variances of most of the coefficients.

2.4 Analysis of the reversible DH schemes

In this subsection we would like to point out the major constraints of the data hiding schemes based on DE and HS embeddings described above. The provided summary will clarify and simplify various aspects that need to be addressed in order to develop the scheme that can outperform the state-of-the-art watermarking techniques and achieve high payload versus quality behavior. So, all the mentioned below data hiding schemes aim at improving some or all of the following aspects:

1. Increasing the amount of payload.
2. Decreasing the redundant data.
3. Improving computational efficiency.

Let us go through the items consequently, and summarize what other researchers have developed. Moreover, it is important to outline the main contributions of our proposed schemes that address the following goals.

In order to increase the amount of payload, various techniques were developed [24]-[29]. One of the methods suggested by Tian implies multiple layer embedding, where the pairing is done in a different direction for each run of the algorithm. However, image quality degrades substantially after the first layer embedding along with the decrease of

embedding capacity of the image. Moreover, every pass reduces the correlation of the neighborhood, and therefore, this approach can no longer embed a high amount of payload without degrading the quality of the image. Among various existing methods which target to improve the capacity limit, there is no scheme that can hide more that one bit per pixel in a single run of the algorithm without bringing high degradation. Therefore, in order to reach high payload capacity, we suggest considering the secret data with elements from Galois field $GF(q)$, $q \geq 2$. The following technique allows to embed more than one bit per pixel in a single run of the algorithm while preserving a sufficient quality of a stego image. Moreover, the amount of payload can be increased by taking an advantage of local activity indicator (LAI), which implies some measure of statistical dispersion. By bounding it with two thresholds we can select only the to be-embedded pixel values. Our generalized scheme allows to implement HS and DE schemes individually, or both of them simultaneously in order to increase the embedding capacity up to 1 bpp in a binary case. On specifying the pairs of valid thresholds of LAI it is possible to choose the to-be-embedded image frequencies along with the data hiding scheme. In the experimental part the scheme's performance behavior for different variations of LAI thresholds is presented in detail.

The auxiliary data comprises the header file that usually is of several hundred bits in addition to illustrative information such as overflow location map, which is necessary for data recovery and has to be compressed not to degrade the capacity limit. As a result, lots of research has been done to decrease its influence on embedding capacity. In [14] Thodi overcame this problem by utilizing a payload-independent overflow LM. However, the scheme does not work well in texture images, where the compressibility of LM is low. In [34] the locations of expanded values are found by statistical analysis. Unfortunately, some additional data should be transmitted to extract the original image and the secret data. The interested reader can find various developed techniques in [35, 36] that target to decrease the auxiliary data, individually. The proposed approach is to derive special conditions for location map free data embedding. However, to obtain the following conditions that allow embedding the data with no redundant information, one additional iteration of the encoding process should be performed. Note that the algorithm allows to leave out this pre-phase in obtaining the conditions. In that case only a single pass of the scheme is conducted with the utilization of losslessly compressed mask, that indicates non-embeddable pixel positions.

In data hiding methods based on the prediction operation, the choice of the predictor contributes a great deal to the performance of the scheme. The prediction errors can be the feature elements used for expansion in DE schemes, while the utilization of prediction error histograms, which contain higher peaks, can achieve a higher payload. Note that the major advantage of the predictor is that it generates the feature elements that have smaller magnitudes, which primarily results in less distortion. We introduce the weighted simplified predictor (WSP) which was designed in [3] that estimates the targeted pixel,

considering its closest neighboring pixels and taking the weighted average of them. Such an approach provides improvement in terms of computational efficiency, that is shown in the experimental part. Therefore, most of the experiments are conducted utilizing WSP predictor; however, it should be noted that the proposed method is invariant to the choice of the predictor and can be performed with any of them.

2.5 Research goals

The performed research on data hiding had the major goal to propose a data-hiding algorithm that addresses limitations and constraints defined in the previous subsection, including the minor goals all of which have been reached:

- Find the thresholds that allow data hiding with no overhead information, i.e. location map free data embedding is achieved.
- Develop a new weighted simplified predictor, which can achieve an improvement in terms of computational costs.
- Use local activity indicator to choose the target embedding image frequencies, which makes the scheme flexible.
- Represent the secret message as elements from Galois field to achieve the capacity of more than 1 bit per pixel in a single run of an algorithm.
- Extend the proposed data-hiding technique to the transform domain complaint with JPEG coding.

All in all, the scheme provides a general, flexible data-hiding approach that targets for the maximum available data embedding capacity without bringing visible distortions and artifacts, and seeking to improve the computational efficiency. Our proposed DE scheme is shown in Figure 8. Here we restrict the generalized scheme only to DE embedding for simplicity of stressing the main contributions, which are underlined. However, the scheme will remain the same for HS and DE+HS embeddings with variation only in the technique of data hiding. The goals presented here also correspond to the timeline of the performed research work. In the following sections all of them will be addressed.

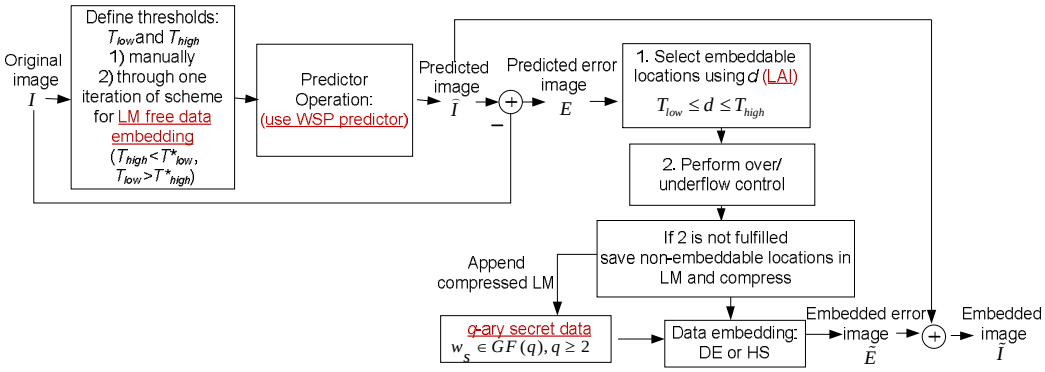

Figure 8: The proposed generalized scheme with only DE embedding (for simplicity) to emphasize the contributions

3 Proposed data embedding schemes

In this section the proposed data embedding approach based on difference expansion and histogram shifting is discussed in detail.

3.1 Difference expansion q-ary approach (q-aryDE)

Let $\mathbf{I} = [I_{i,j}]$ denote a cover $M \times N$ image, $W = \{w_s\}$ be a secret data with elements from Galois field, $w_s \in GF(q)$. Here and further, $i = \overline{0,M-1}$, $j = \overline{0,N-1}$, $w_s = \overline{0,q-1}, s = \overline{1,S}$. Assume $\widehat{I}_{i,j}$ to be the predicted pixel at the spatial location (i,j), and $\Omega_{i,j}$ - a causal window (region) used for a local prediction of the pixel at position (i,j). Note that the scheme can be performed with any chosen predictor. The prediction error at position (i,j) is defined by:

$$E_{i,j} = I_{i,j} - \widehat{I}_{i,j}. \tag{19}$$

We introduce $d_{i,j}$, a local activity indicator, that allows to select only the to-be-embedded pixels. Let $d_{i,j}$ be a measure of some statistical dispersion, for example, a maximum absolute deviation computed over the region $\Omega_{i,j}$:

$$d_{i,j} = \max \mid \Omega_{i,j} - \text{mean}(\Omega_{i,j}) \mid . \tag{20}$$

In order to control embedding of secret data, we introduce two user-specified parameters T^{DE}_{low} and T^{DE}_{high} :

$$T^{\text{DE}}_{low} \leq d_{i,j} \leq T^{\text{DE}}_{high}. \tag{21}$$

If condition (21) is not fulfilled, we consider the region $\Omega_{i,j}$ as complex, where the prediction error does not have a small magnitude, therefore, contributes no payload. To decrease unnecessary pixel modification, LAI skips the pixel $I_{i,j}$. The inequality (22) employs under/overflow control to prevent the values from exceeding the range $[0, K-1]$, where $K = 2^k$ is a number of the image levels, for example, $K = 256$ for 8-bit grayscale images:

$$q \leq \widehat{I}_{i,j} + q * E_{i,j} \leq K - 1 - q. \tag{22}$$

3.1.1 Data embedding

The embedding is done according to the following equation:

$$\tilde{I}_{i,j} = \begin{cases} \widehat{I}_{i,j} + qE_{i,j} + w_s, & \text{if (21) and (22) are fulfilled,} \\ I_{i,j}, & \text{otherwise,} \end{cases} \tag{23}$$

where $w_s \in GF(q)$. A set of coordinates (i,j), for which (21) is fulfilled but (22) is not, forms a set of non-embeddable pixel positions. A mask indicating these positions is losslessly compressed and used as a location map to be appended to the secret data for

embedding. We define two integer valued matrices $\mathbf{L} = [l_{i,j}]$ and $\mathbf{U} = [u_{i,j}]$ as follows:

$$l_{i,j} = \begin{cases} \infty, & \text{if (22) is fulfilled,} \\ d_{i,j}, & \text{otherwise,} \end{cases} \tag{24}$$

$$u_{i,j} = \begin{cases} 0, & \text{if (22) is fulfilled,} \\ d_{i,j}, & \text{otherwise,} \end{cases} \tag{25}$$

with corresponding minimum and maximum values:

$$T^*_{low} = \min_{i,j} l_{i,j}; T^*_{high} = \max_{i,j} u_{i,j}. \tag{26}$$

Proposition 1. A set of non-embeddable pixel positions is empty, or, in other words, the embedding process defined by (23) is a location map-free iff $T^{\mathrm{DE}}_{high} < T^*_{low}$ or $T^{\mathrm{DE}}_{low} > T^*_{high}$, where T^{DE}_{low} and T^{DE}_{high} are user specified parameters in (21), and T^*_{low} and T^*_{high} are defined in (26).

Proof. Let us assume the contrary, that $T^{\mathrm{DE}}_{high} < T^*_{low}$ or $T^{\mathrm{DE}}_{low} > T^*_{high}$, but condition (22) is not fulfilled, i.e. the set of non-embeddable pixels is not empty. Then, from (24) and (26) we have:

$$T^*_{low} \le d_{i,j} \le T^*_{high}, \tag{27}$$

keeping in mind that (22) is not fulfilled, which is illustrated in Figure 9(a). Since the embedding is done when $T^{\mathrm{DE}}_{low} \le d_{i,j} \le T^{\mathrm{DE}}_{high}$, then, if $T^{\mathrm{DE}}_{high} < T^*_{low}$ or $T^{\mathrm{DE}}_{low} > T^*_{high}$, the following inequalities of data embedding intervals are also true: $T^{\mathrm{DE}}_{low} \le d_{i,j} < T^*_{low}$ or $T^*_{high} < d_{i,j} \le T^{\mathrm{DE}}_{high}$ as it follows from (27) and shown in Figure 9(b).

Since two pairs of conditions $T^*_{low} \le d_{i,j}$ but $d_{i,j} < T^*_{low}$ as well as $d_{i,j} \le T^*_{high}$ but $T^*_{high} < d_{i,j}$ are contradicting, the assumption is wrong, and the proposition is proven.

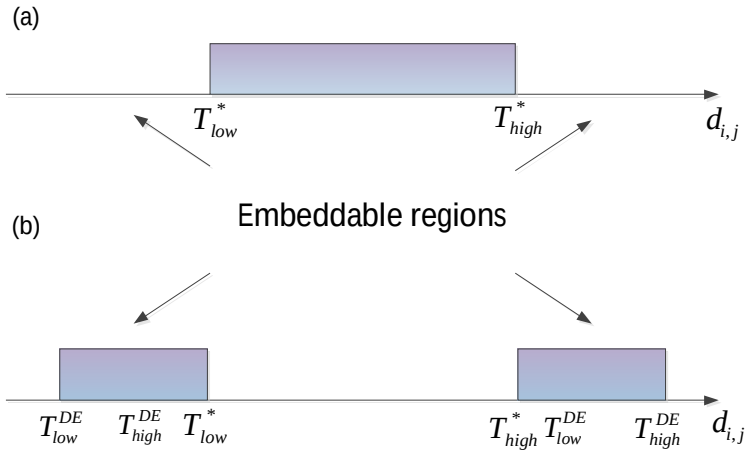

Figure 9: The illustration of the proposition 1

3.1.2 Host image and hidden q-ary data extraction

Similarly to the data embedding process causal prediction is utilized at the reconstruction stage. Therefore, the new prediction error is found:

$$E_{i,j}^{new} = \tilde{I}_{i,j} - \widehat{I}_{i,j}, \tag{28}$$

and the maximum absolute deviation $d_{i,j}$ similar to (19) and (20) are computed. The forthcoming proposition reveals the process of extracting the hidden data and reconstructing the original host image.

Proposition 2. Assume $\tilde{\mathbf{I}}$ and $\widehat{\mathbf{I}}$ to be the watermarked and the predicted images, respectively, and $E_{i,j}^{new}$ to be a new prediction error (28). The hidden message w_s and the original host image $\mathbf{I}$ can be extracted by the following formulas:

$$w_s = E_{i,j}^{new} \mathrm{mod} q, \tag{29}$$

$$I_{i,j} = \widehat{I}_{i,j} + \frac{E_{i,j}^{new} - w_s}{q}, \tag{30}$$

if (21) and (22) are both fulfilled, and $I_{i,j} = \tilde{I}_{i,j}$, otherwise.

Proof. Since embedding is done only if conditions (21) and (22) are satisfied, we have to prove only (29) and (30). Formula (29) is derived from the embedding procedure, $E_{i,j}^{new} = qE_{i,j} + w_s$. On taking modulo q we obtain w_s. The original image can be reconstructed by finding $E_{i,j}$ from $E_{i,j}^{new}$. Therefore, $qE_{i,j} = E_{i,j}^{new} - w_s$, or $E_{i,j} = (E_{i,j}^{new} - w_s)/q$. On substituting $E_{i,j}$ into $I_{i,j} = \hat{I}_{i,j} + E_{i,j}$ we arrive to (30).

In order to clarify the DE algorithm introduced above, we consider a simple example of embedding four bits in a binary representation $w_s = \{1,0,1,1\}$ into the 3×3 image $\mathbf{I}$, presented in Figure 10. We explain descriptively the hiding and extraction processes of the first bit into $I_{2,2}$, while the same procedures are conducted analogously for the rest of the pixels. In our predictor-invariant technique we choose MED defined in [19] to be utilized for calculation of the prediction. Note that both first row and column remain unchanged, according to the specified local MED prediction area $\Omega_{2,2}$, which is marked with gray color in the center image. Therefore, the first predicted pixel is $\widehat{I}_{2,2} = 10$. The next step includes calculating the LAI $d_{2,2} = \max \mid \Omega_{2,2} - \mathrm{mean}(\Omega_{2,2}) \mid = 0.67$, and obtaining the prediction error $E_{2,2} = I_{2,2} - \widehat{I}_{2,2} = 1$. We verify the two conditions (21) and (22) : $0 \leq d_{2,2} \leq 2$, $2 \leq \widehat{I}_{2,2} + 2 * E_{2,2} \leq 253$, which are correct, and, therefore, perform the embedding operation $\tilde{I}_{i,j} = 10 + 2 * 1 + 1 = 13$.

At the extraction phase, a similar routine is applied to the watermarked image $\tilde{\mathbf{I}}$, which we reveal in terms of pixel $I_{2,2}$. After finding prediction pixel $\widehat{I}_{2,2} = 10$ using MED prediction strategy and statistical dispersion $d_{2,2} = 0.67$, we compute the new prediction error $E_{2,2}^{new} = \tilde{I}_{2,2} - \widehat{I}_{2,2} = 3$ and verify conditions (21) and (22), the correctness of which lead us to obtain the secret bit $w_1 = E_{2,2}^{new} \mathrm{mod} 2 = 1$ and the original pixel $I_{2,2} = \widehat{I}_{2,2} +$

$\frac{E^{new}_{2,2}-w_1}{q} = 10+(3-1)/2 = 11.$

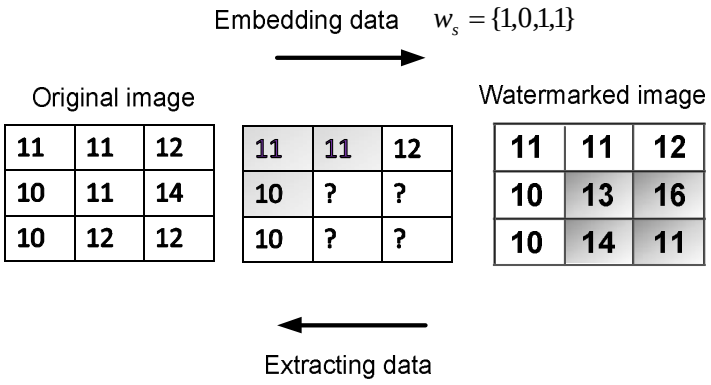

Figure 10: Example of the proposed DE embedding scheme, $q = 2$, $[T^{\mathrm{DE}}_{low}, T^{\mathrm{DE}}_{high}] = [0,2]$

3.2 Histogram shifting q-ary approach (q-aryHS)

This section presents the extension of the method, described above, based on LAI, which utilizes histogram shifting instead of the difference expansion approach, resulting in higher embedding capacity. The data hiding process is controlled by two user specified thresholds T^{HS}_{low} and T^{HS}_{high}, similarly to DE method, which are defined by:

$$T^{\mathrm{HS}}_{low} \leq d_{i,j} \leq T^{\mathrm{HS}}_{high}. \tag{31}$$

Let us apply one more control mechanism, enabling the data embedding process only if the prediction error is bounded:

$$E_{i,j} \in [-Q, Q], \tag{32}$$

where $Q \geq 0$ is a user-specified parameter. In order to employ over/underflow control to prevent the values from exceeding the range $[0, K-1]$, where K is a number of the image levels, the special condition is presented:

$$\begin{cases} 0 \leq \widehat{I}_{i,j} + E_{i,j} - (q-1)Q \leq K-1, & \text{if } E_{i,j} < -Q, \\ 0 \leq \widehat{I}_{i,j} + qE_{i,j} \leq K-1, & \text{if } -Q \leq E_{i,j} < 0, \\ 1 \leq \widehat{I}_{i,j} + q(E_{i,j}+1) \leq K, & \text{if } 0 \leq E_{i,j} < Q, \\ 0 \leq \widehat{I}_{i,j} + E_{i,j} + (q-1)Q \leq K-1, & \text{if } E_{i,j} \geq Q. \end{cases} \tag{33}$$

3.2.1 Data embedding

The embedding is done according to the following formula:

$$\tilde{I}_{i,j} = \begin{cases} \widehat{I}_{i,j} + E_{i,j} - (q-1)Q, & \text{if } E_{i,j} < -Q, \\ \widehat{I}_{i,j} + q(E_{i,j}+1) - w_s - 1, & \text{if } -Q \le E_{i,j} < 0, \\ \widehat{I}_{i,j} + qE_{i,j} + w_s, & \text{if } 0 \le E_{i,j} < Q, \\ \widehat{I}_{i,j} + E_{i,j} + (q-1)Q, & \text{if } E_{i,j} \ge Q, \end{cases} \tag{34}$$

if (33) is accomplished. A set of coordinates (i, j) for which (31) is fulfilled but (33) is not, forms a set of non-embeddable pixel positions. Note that the scenario for $Q = 1$, $q = 2$ corresponds to the embedding technique introduced in [29]. Here we propose a generalized scheme for an arbitrary Q. Apparently, by increasing the value of Q while accomplishing (33), we can achieve a higher embedding capacity, which will be demonstrated in the experimental part. Note that the scheme implies the search of the thresholds T^{HS}_{low} and T^{HS}_{high} for LM free data embedding, analogously to the DE case. Therefore, the similar to (24) and (25), matrices are obtained with the corresponding minimum and maximum values as in (26). Hence, we derive the following proposition (similar to proposition 1), which defines the conditions for location map free data embedding.

Proposition 3. A set of non-embeddable pixel positions is empty, or in other words, the embedding process defined by (34) is a location map-free iff $T^{\mathrm{HS}}_{high} < T^{*}_{low}$ or $T^{\mathrm{HS}}_{low} > T^{*}_{high}$, where T^{HS}_{low} and T^{HS}_{high} are obtained from (31), and T^{*}_{low} and T^{*}_{high} are defined in (26).

The proof of the proposition 3 is done analogously to the proof of the proposition 1.

Note that one additional iteration of the algorithm is required to obtain the thresholds for HS location map free data embedding, which can help substantially decrease the auxiliary data. However, the step can be omitted by utilizing user-specified conditions T^{HS}_{low}, T^{HS}_{high} within the algorithm.

3.2.2 Host image and hidden q-ary data extraction

At the reconstruction stage similarly to the embedding process, a causal prediction is used, a new prediction error $E^{new}_{i,j}$ specified in (28) and $d_{i,j}$ defined in (20) are computed. The extraction of the hidden data and reconstruction of an original host image is presented in the following proposition.

Proposition 4. Let $\tilde{I}_{i,j}$ and $\widehat{I}_{i,j}$ be the watermarked and the predicted image pixels, respectively. The hidden message w_s and original host image $I_{i,j}$ can be extracted by

$$w_s = \begin{cases} (-E^{new}_{i,j} - 1) \bmod q, & \text{if } -qQ \le E^{new}_{i,j} < 0, \\ E^{new}_{i,j} \bmod q, & \text{if } 0 \le E^{new}_{i,j} < qQ. \end{cases} \tag{35}$$

$$I_{i,j} = \begin{cases} \widehat{I}_{i,j} + E_{i,j}^{new} + (q-1)Q, & \text{if } E_{i,j}^{new} < -qQ, \\ \widehat{I}_{i,j} + (E_{i,j}^{new} + w_s + 1)/q - 1, & \text{if } -qQ \le E_{i,j}^{new} < 0, \\ \widehat{I}_{i,j} + (E_{i,j}^{new} - w_s)/q, & \text{if } 0 \le E_{i,j}^{new} < qQ, \\ \widehat{I}_{i,j} + E_{i,j}^{new} - (q-1)Q, & \text{if } E_{i,j}^{new} \ge qQ, \end{cases} \tag{36}$$

if (31) and (33) are both fulfilled, and $I_{i,j} = \tilde{I}_{i,j}$, otherwise.

Proof. According to the embedding procedure a new prediction error is equal to $E_{i,j}^{new} = qE_{i,j} + w_s$, where $E_{i,j}$ is a prediction error before embedding, if $0 \le E_{i,j}^{new} < qQ$; thus, in this case $w_s = E_{i,j}^{new} \text{mod} q$. The reconstructed image can be obtained by adding a predicted image $\widehat{I}_{i,j}$ to the old prediction error $E_{i,j}$ (since $E_{i,j} = I_{i,j} - \widehat{I}_{i,j}$), $I_{i,j} = \widehat{I}_{i,j} + E_{i,j} = \widehat{I}_{i,j} + (E_{i,j}^{new} - w_s)/q$. Similarly, if $-qQ \le E_{i,j}^{new} < 0$, a new prediction error is equal to $E_{i,j}^{new} = qE_{i,j} + q - w_s - 1$. Thus, $w_s = (-E_{i,j}^{new} - 1) \text{mod} q$. In that case, $I_{i,j} = \widehat{I}_{i,j} + E_{i,j} = \widehat{I}_{i,j} - 1 + (E_{i,j}^{new} + w_s + 1)/q$. Since $E_{i,j}^{new} = E_{i,j} + (q-1)Q$, when $E_{i,j} \ge Q$; therefore, for $E_{i,j}^{new} \ge qQ$ we have $E_{i,j} = E_{i,j}^{new} - (q-1)Q$. Similarly, since $E_{i,j}^{new} = E_{i,j} - (q-1)Q$, when $E_{i,j} < -Q$, for $E_{i,j}^{new} < qQ$ we have $E_{i,j} = E_{i,j}^{new} + (q-1)Q$, which concludes the proof.

Let us consider a simple example of the proposed HS embedding procedure of hiding eight bits in a 4-ary representation $w_s = \{3,0,1,1\}$ into the cover 3×3 image $\mathbf{I}$, presented in Figure 11. Here, the thresholds $[T_{low}^{\text{HS}}, T_{high}^{\text{HS}}] = [0,2]$ and $Q = 3$. We will clarify as before only the embedding and extraction of the first two bits into $I_{2,2}$ utilizing the same MED predictor. The predicted pixel is $\widehat{I}_{2,2} = 10$. When calculating the LAI we get $d_{2,2} = 0.67$, and the prediction error $E_{2,2} = I_{2,2} - \widehat{I}_{2,2} = 1$. We verify the two conditions (31) and (33), which are correct, and, therefore, perform the embedding operation $\tilde{I}_{i,j} = \widehat{I}_{i,j} + qE_{i,j} + w_1 = 10 + 4 * 1 + 3 = 17$.

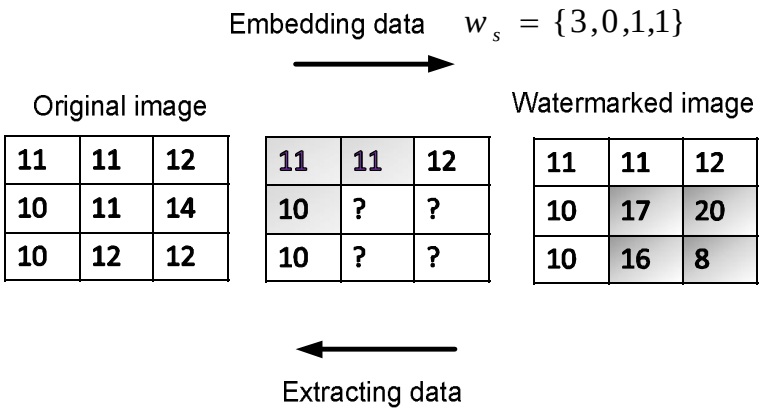

Figure 11: Example of the proposed HS embedding scheme, $q = 4$, $[T_{low}^{\text{HS}}, T_{high}^{\text{HS}}] = [0,2]$, $Q = 3$

At the extraction phase, a similar routine is applied to the watermarked image $\tilde{\mathbf{I}}$. After

finding prediction pixel $\widehat{I}_{2,2} = 10$ using MED prediction strategy and statistical dispersion $d_{2,2} = 0.67$, we compute new prediction error $E_{2,2}^{new} = \tilde{I}_{2,2} - \widehat{I}_{2,2} = 7$ and verify conditions (31) and (33), correctness of which lead us to obtain the secret bit $E_{i,j}^{new} \bmod q = 3$ and the original pixel $I_{2,2} = \widehat{I}_{i,j} + (E_{i,j}^{new} - w_1)/q = 10 + (7-3)/4 = 11$.

3.3 Mixed q-ary HS and DE algorithm

In the previous subsections two algorithms were described, which were realized and investigated in [2, 3]. Note that the schemes differ only in the embedding procedure, while the general approach of the proposed data-hiding algorithm is the same. Therefore, to achieve a higher payload when performing the embedding to both low and high frequency components, both DE and HS schemes can be used simultaneously. The generalized scheme allows to perform each of the embeddings separately, by leaving out the unnecessary thresholds, or utilize both watermarking schemes at once. Therefore, when varying the thresholds T_{low}^{DE}, T_{high}^{DE} and T_{low}^{HS}, T_{high}^{HS} different combinations of the proposed data embedding algorithm can be obtained. The mixed algorithm comprises three stages: pre-encoding (optional), encoding and image reconstruction.

1) *Pre − encoding stage*. This stage implies an iteration of the encoding process of the proposed scheme in order to find the pairs of thresholds $T_{low}^{\mathrm{DE}^*}$, $T_{high}^{\mathrm{DE}^*}$ and $T_{low}^{\mathrm{HS}^*}$, $T_{high}^{\mathrm{HS}^*}$ that control the embedding capacity for location map free data embedding. The pre-encoding stage in Figure 12 comprises the step-by-step description of how the thresholds are obtained. Note that one additional iteration of the encoding process is required to identify the thresholds that allow embedding the data with no redundant information and can substantially increase the payload. However, the algorithm allows to leave out the computation of thresholds by specifying the initially user selected thresholds T_{low}^{DE}, T_{high}^{DE} and T_{low}^{HS}, T_{high}^{HS}. In that case, only one iteration of the algorithm is performed with the utilization of a losslessly compressed mask, that indicates non-embeddable pixel positions.

2) *Embedding stage*. The data embedding procedure is implemented for a predefined predictor and thresholds that specify the embedding frequency components and data hiding technique. Therefore, the predicted pixel $\widehat{I}_{i,j}$ at the spatial location (i, j) and the prediction error $E_{i,j}$ obtained using (19) are calculated. The maximum absolute deviation, used as a measure of statistical dispersion, is computed via (20). When verifying the conditions the given type of the embedding, or both of them, is performed. Figure 13 presents the main steps of the embedding procedure.

3) *Reconstruction stage*. Image and secret data extraction is done similarly to the embedding process. Before performing the data extraction, the predicted pixel, the new prediction error defined by (28) and the maximum absolute deviation are restored. The extraction of the hidden data is conducted according to proposition 2 or 4 depending on the embedding scheme. The original image is losslessly resumed as soon as the embedded secret message is completely extracted.

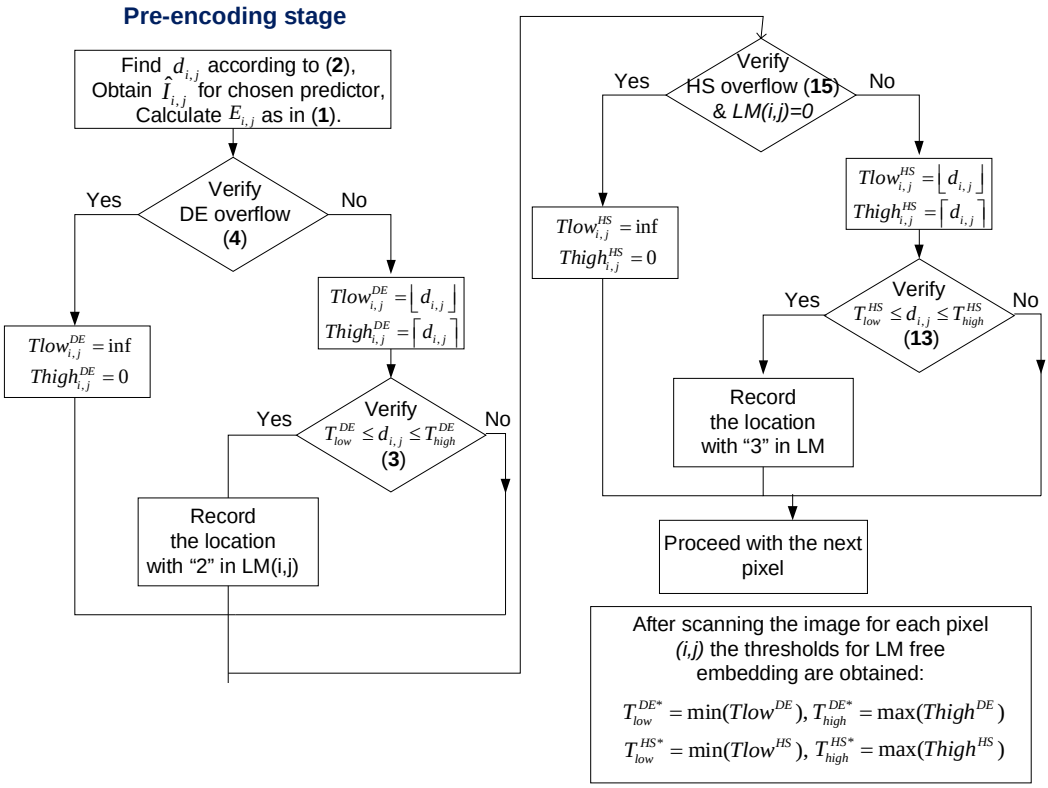

Figure 12: Pre-encoding stage of the proposed generalized scheme

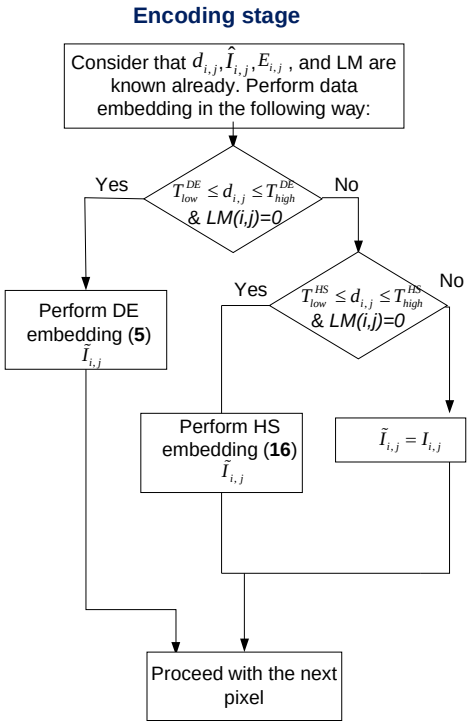

Figure 13: Encoding stage of the proposed generalized scheme. Reconstruction stage is conducted analogously to the embedding process

4 Extension to JPEG data hiding

The developed DE and HS embedding techniques operate efficiently in the spatial domain. Keeping in mind that JPEG standard is the most commonly used digital image standard nowadays, since it achieves a high compression ratio while retaining sufficient image quality, we propose to extend the introduced data embedding schemes to the DCT frequency domain. The block diagram of the proposed data hiding JPEG codec is shown in Figure 14. The digital image used as the cover signal is decomposed into a set of 8×8 blocks, then DCT is computed, after which the transformed coefficients are quantized using a JPEG standard quantization table, which is displayed in Figure 15.

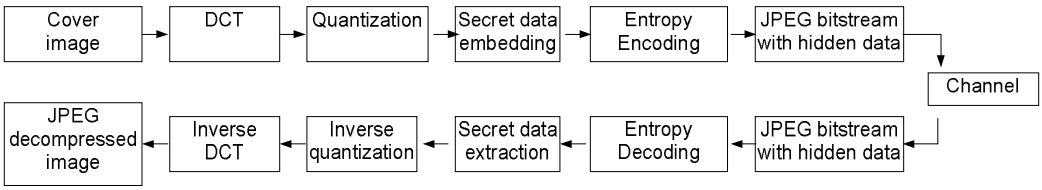

Figure 14: Block diagram of data hiding in JPEG codec

16	11	10	16	24	40	51	61
12	12	14	19	26	58	60	55
14	13	16	24	40	57	69	56
14	17	22	29	51	87	80	62
18	22	37	56	68	109	103	77
24	35	55	64	81	104	113	92
49	64	78	87	103	121	120	101
72	92	95	98	112	100	103	99

Figure 15: Default quantization table of JPEG encoder

The secret data in q-ary representation is then embedded into the quantized coefficients and coded by using the combination of run-length and Huffman encoding. At the decoder, the inverse procedures are conducted: after Huffman decoding the secret data from the DCT quantized coefficients is extracted and inverse DCT is performed. The final decompressed JPEG image is obtained after rounding the values.

Data hiding in frequency domain imposes a number of constraints on the embedding techniques: decompression/recompression both introduce distortion to the image, reduce its quality and vary the statistics of the DCT coefficients in the JPEG stream, which is not suitable for steganography applications. Moreover, such techniques are usually computationally more expensive than those which do not require decompression. Therefore,

we analyze a data hiding scheme that performs data embedding and extraction directly without decompression.

4.1 Data embedding approach

Data embedding is performed on the zig-zag ordered quantized DCT coefficients $b_{m,n} = \{c^1_{m,n}, ..., c^{64}_{m,n}\}$, where $m = \overline{1,M'}, n = \overline{1,N'}$, and M', N' are the total numbers of 8×8 blocks in horizontal and vertical directions, respectively. We organize separate AC_k planes by taking k DCT coefficients from every block. Here and further, $k = \overline{1,64}$:

$$AC_k = \begin{bmatrix} c^k_{1,1} & \cdots & c^k_{1,N'} \\ \vdots & & \vdots \\ c^k_{M',1} & \cdots & c^k_{M',N'} \end{bmatrix}. \tag{37}$$

We separate DCT coefficients into individual AC planes and apply the embedding technique described above. Note that HS data hiding approach that uses error control parameter allows a higher flexibility, which reflects the performance of the scheme. In our HS embedding scheme the prediction error was bounded by the interval $[-Q, Q)$, where Q specifies the bins utilized for embedding, being symmetric with respect to 0. Here we generalize the target interval to be symmetric with respect to h: $[-Q-h, -h) \cap [h, h+Q)$. Adding the new parameter h allows us to improve DH scheme's flexibility by leaving out embedding into zeros, which in terms of AC components easily bring visual changes and can significantly increase the file size. Note that operating in the frequency domain enables to omit employing under/overflow control, and when verifying (31), we perform embedding in a slightly different way with respect to the introduced parameter h:

$$\tilde{I}_{i,j} = \begin{cases} \widehat{I}_{i,j} + E_{i,j} - (q-1)Q, \text{if } E_{i,j} < -Q-h, \\ \widehat{I}_{i,j} + q(E_{i,j}+1) - w_s - 1 + h(q-1), \text{if } -Q-h \le E_{i,j} < -h, \\ \widehat{I}_{i,j} + qE_{i,j} + w_s - h(q-1), \text{if } h \le E_{i,j} < h+Q, \\ \widehat{I}_{i,j} + E_{i,j} + (q-1)Q, \text{if } E_{i,j} \ge Q+h. \end{cases} \tag{38}$$

4.2 Data extraction approach

At the extraction phase after Huffman decoding, we operate on quantized DCT coefficients, which are separated into the individual AC planes. Huffman coding is a lossless operation; therefore, after recovering the secret message, we can get back the JPEG de-

compressed image, as follows:

$$w_s = \begin{cases} ((h(q-1)-1)\text{mod}q - E)\text{mod}q, & \text{if} \\ -h - qQ \leq E_{i,j}^{new} < -h, & \\ ((h(q-1))\text{mod}q + E)\text{mod}q, & \text{if} \\ h \leq E_{i,j}^{new} < h + qQ - 1, & \end{cases} \tag{39}$$

$$I_{i,j} = \begin{cases} \widehat{I}_{i,j} + E_{i,j}^{new} + (q-1)Q, & \text{if} \\ E_{i,j}^{new} < -qQ - h, & \\ \widehat{I}_{i,j} + (E_{i,j}^{new} + w_s + 1 - h(q-1))/q - 1, & \text{if} \\ -h - qQ \leq E_{i,j}^{new} < -h, & \\ \widehat{I}_{i,j} + (E_{i,j}^{new} - w_s + h(q-1))/q, & \text{if} \\ h \leq E_{i,j}^{new} < h + qQ - 1, & \\ \widehat{I}_{i,j} + E_{i,j}^{new} - (q-1)Q, & \text{if} \\ E_{i,j}^{new} \geq qQ + h. & \end{cases} \tag{40}$$

Selection of the DCT coefficients is one of the issues that is to be addressed when using the quantized DCT coefficients for data hiding. Keeping in mind that varying DC components can easily cause blocking artifacts, we consider AC counterparts to be the candidate for data hiding. Particularly, the choice of high frequency AC components used for embedding will lead to visually significant changes. Therefore, to apply the embedding procedure to high frequency AC coefficients, modifications to the quantization tables are required to be conducted, since their quantization steps are the largest. Finally, the modified quantization table has to be sent to the decoder in the standard JPEG stream header. In order to exclude the given redundant information, in our scheme we will utilize mid-frequency components of each of the DCT block along with the standard quantization table of JPEG. Note that JPEG default table can be scaled to a quality factor Q_f, the value of which ranges from 0 to 100. The description of the scaling procedure can be found in [37].

The elaborated technique of HS embedding has the freedom to control the distortion and valuable payload by changing a number of parameters: quality factor of the quantization operation Q_f, embeddable AC components AC_k, prediction error control parameters Q, h. Considering the transmission of JPEG format images, we can assume that the payload can be concatenated with the cover data itself. Although the following approach is not sustainable to the sniffing types of attacks, it helps us to narrow the parameter specification, which simplifies the experimental analysis, by selecting only the embeddable AC components, for which the following property is fulfilled:

The size of JPEG bitstream after Huffman encoding plus the secret message is more than the size of JPEG watermarked bitsream.

Although the procedure is computationally expensive, a number of embeddable AC components that are capable of effective embedding without enlarging the image size significantly are obtained. Note that in that case the payload should not be very high; therefore, we also conduct a round of experiments for a user-specified AC components with a small increase in file size. In the experimental part the extended to JPEG images scheme is compared to a number of state-of-the-art algorithms [32, 33] and it is shown that the scheme provides high embedding capacity without detectable visual artifacts.

5 Performance evaluation results

5.1 Predictors chosen for implementation

A predictor operates on a neighborhood of a given pixel in order to predict its value. It is desirable to have the smallest magnitudes of the prediction errors, because they are used for expansion in DE schemes, and contain higher peaks prediction error histograms in HS schemes. Therefore, the choice of the pixel's neighborhood may influence substantially on the quality of the stego image. Below the used in the experimental part local predictors that operate in the area of to-be predicted pixel are defined. MED predictor is the one example that can exploit the neighboring information to predict an image pixel [19]:

$$\widehat{I}_{i,j} = \begin{cases} \max(a,b), & \text{if } c \leq \min(a,b), \\ \min(a,b), & \text{if } c \geq \max(a,b), \\ a+b-c, & \text{otherwise,} \end{cases} \tag{41}$$

where $a = I_{i,j-1}$, $b = I_{i-1,j}$, and $c = I_{i-1,j-1}$. It uses raster scan order and applies edge rule to evaluate the predicted pixel. The GAP predictor operates on seven neighbors of the current pixel of the cover image $I_{i,j}$.

$$\begin{aligned} d_h &= \mid I_{i-1,j} - I_{i-2,j} \mid + \mid I_{i,j-1} - I_{i-1,j-1} \mid + \\ &\quad \mid I_{i,j-1} - I_{i+1,j-1} \mid, \end{aligned}$$

$$\begin{aligned} d_v &= \mid I_{i-1,j} - I_{i-1,j-1} \mid + \mid I_{i,j-1} - I_{i,j-2} \mid + \\ &\quad \mid I_{i+1,j-1} - I_{i+1,j-2} \mid, \end{aligned}$$

$$D = d_v - d_h,$$

$$J_{i,j} = (I_{i-1,j} + I_{i,j-1})/2 + (I_{i+1,j-1} + I_{i-1,j-1})/4,$$

$$\widehat{I}_{i,j} = \begin{cases} I_{i,j-1}, & \text{if } D < -80, \\ (J_{i,j} + I_{i,j-1})/2, & \text{if } -80 \leq D < -32, \\ (3J_{i,j} + I_{i,j-1})/4, & \text{if } -32 \leq D < -8, \\ J_{i,j}, & \text{if } -8 \leq D < 8, \\ (3J_{i,j} + I_{i-1,j})/4, & \text{if } 8 \leq D < 32, \\ (J_{i,j} + I_{i-1,j})/2, & \text{if } 32 \leq D < 80, \\ I_{i-1,j}, & \text{if } D \geq 80. \end{cases} \tag{42}$$

The weighted simplified predictor (WSP) operates on the neighboring pixels: $\Omega_{i,j} = (I_{i-1,j}, I_{i,j-1}, I_{i-1,j+1})$ [3]. First, directional differences are computed as Euclidean dis-

tance between the pixel value $I_{i,j}$ and all $\Omega_{i,j}$ elements:

$$\widehat{\Omega}_{i,j}(k) = \mid I_{i,j} - \Omega_{i,j}(k) \mid . \tag{43}$$

Here and further, $k = \overline{1,3}$. For every element in $\Omega_{i,j}$ we find the maximum value of the directional differences defined as:

$$\widehat{\Omega}'_{i,j}(k) = \max\left(\frac{\widehat{\Omega}_{i-1,j}(k), \widehat{\Omega}_{i,j-1}(k)}{2}\right). \tag{44}$$

The next step is to compute weight coefficients and normalize them:

$$c_{i,j}(k) = 2^{-\widehat{\Omega}'_{i,j}(k)}, c'_{i,j}(k) = \frac{c_{i,j}(k)}{\sum_k (c_{i,j}(k))}. \tag{45}$$

Thus, the predicted pixel can be obtained:

$$\widehat{I}_{i,j} = \sum_k \Omega_{i,j}(k) c'_{i,j}(k). \tag{46}$$

Neighboring pixels are exploited to evaluate the similarity in various directions and adapt the weights accordingly.

Figure 16 shows various neighborhoods of three predictors: MED (solid line), GAP (thick dashed line) and the proposed WSP (thin dashed line). Note that the proposed scheme works well with any predictor including non-local predictors that consider non-local similarity and extend the analysis of the neighboring region to a much larger one [38, 39].

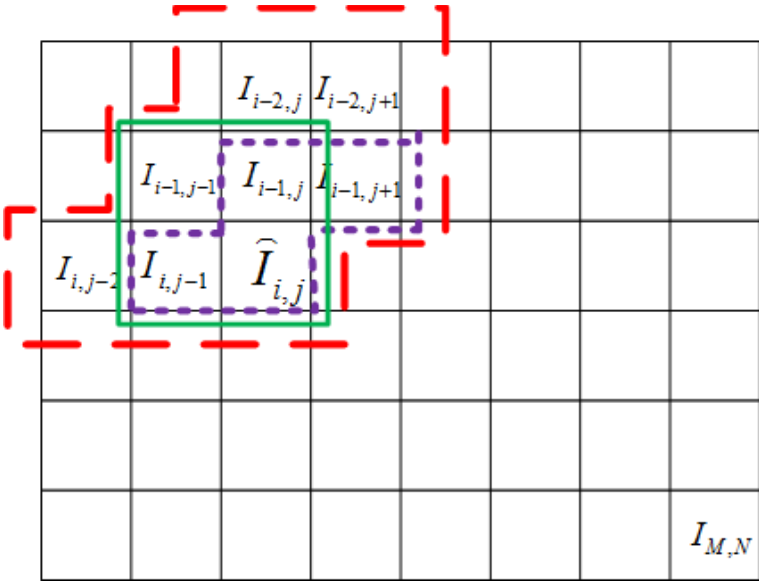

Figure 16: Neighborhoods of three utilized predictors MED (solid line), GAP (thick dashed line) and WSP (thin dashed line)

5.2 Experimental results

This section presents the results of the experimental analysis performed to verify the effectiveness of the proposed data hiding approach. Two sets of images are used. The first one comprises 512×512 grayscale (8-bit) and color (24-bit) test host images taken from the UWaterloo database [40] and shown in Figure 17. These images are frequently used by the researches for their high variation in the statistics, such as a number of uniform areas, texture and contrast. However, to get a more adequate behavior of the scheme, the second set of Kodak test images of good quality is considered. The test set consists of 24-bits images of sizes 512×768, which were released by the Eastman Kodak Company for unrestricted usage [41]. The graylevel versions of the Kodak images are computed and presented in Figure 18. The peak signal-to noise ratio (PSNR) is exploited to measure the stego image quality in dB:

$$\mathrm{PSNR} = 10\log_{10}\frac{(2^k-1)^2}{MSE}, \tag{47}$$

where k is the bit depth for the cover media and MSE is the mean squared error between the cover and the stego images. The payload is measured in bits per pixel (bpp) and is defined by the difference of the capacity of the given cover image and the auxiliary data. Structural similarity (SSIM) allows to efficiently assess the perceptual visual quality of the image [43]. In order to evaluate the performance the q-ary data is converted into binary one by applying the base two logarithm of the q-ary elements. As it was mentioned above, the proposed q-ary scheme is invariant to the choice of the predictor, and therefore, MED, GAP and WSP predictors proposed in [3] are selected for experiments. The MED is a high-performance predictor already used in JPEG-LS standard [19]. The GAP is a major part of context-based, adaptive, lossless image coding (CALIC) algorithm [29]. Their computational complexity comparison can be seen in Table 3, where the predictors in terms of computational costs (number of additions μ_+, multiplications $\mu_\times$, comparisons μ_C and shift operations μ_S) are examined. It is worth mentioning that WSP predictor allows to combine the neighboring pixels and suitably weigh them depending on the directional distances. Moreover, it can achieve a high performance in terms of capacity, quality and complexity, which was revealed in [3]. Thus, WSP is used at the base of the prediction operation. The experimental part is divided in two subsections separated by the spatial and frequency domains to achieve better and clearer perception of the results.

Table 3: Computational complexity per pixel for MED, GAP and WSP predictors

Predictor	μ_+	$\mu_\times$	μ_C	μ_S
MED	2	0	4	0
GAP	18	8	6	0
WSP	5	1	3	6

Figure 17: The 8-bit first set of test images utilized in the experimental part. In the upper row and from left to right: grayscale Mandrill, Lena and Barbara. In the lower row from left to right: grayscale Couple and Man, and Lena in RGB color space

Figure 18: The 8-bit second set of Kodak test images utilized in the experimental part

5.3 The performance of the proposed DH scheme in the spatial domain

The effectiveness of the proposed approach in the spatial domain is assured by the comparison in terms of the embedding capacity versus image quality curves with the histogram modification technique implemented by Xuan [5] and the prediction error expansion reversible watermarking developed by Coltuc [4]. It is worth mentioning that Xuan designed the scheme that outperforms a number of reversible data hiding methods such as [6, 21]. The quality versus payload curves are performed for a set of 512 $\times$ 512 Man, Lena, Barbara and Couple test images and are shown in Figures 19-22, respectively. The user-defined thresholds are set as follows: [T_{low}^{DE}, T_{high}^{DE}]=[0,T] , [T_{low}^{HS}, T_{high}^{HS}]=[0,3T], where $T = [1,3,5,10,15,20,25,40,50,60]$. The Q parameter takes values from 1 to 7. It can be obviously concluded that the proposed 2-aryHS and mixed 2-aryHS+DE methods achieve a higher performance in comparison to Xuan's histogram scheme based on MED and GAP predictors. Note that DE and HS+DE techniques, generally, achieve higher payloads, while HS technique, in turn, produces a better quality performance.

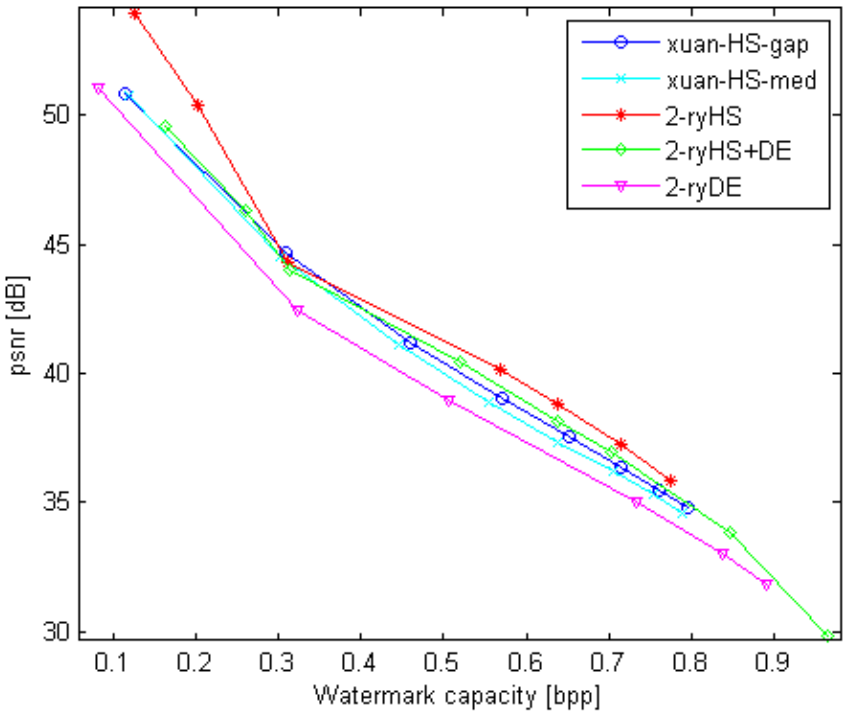

Figure 19: The embedding capacity versus image quality PSNR comparison curve for 512×512 Man, $q = 2$

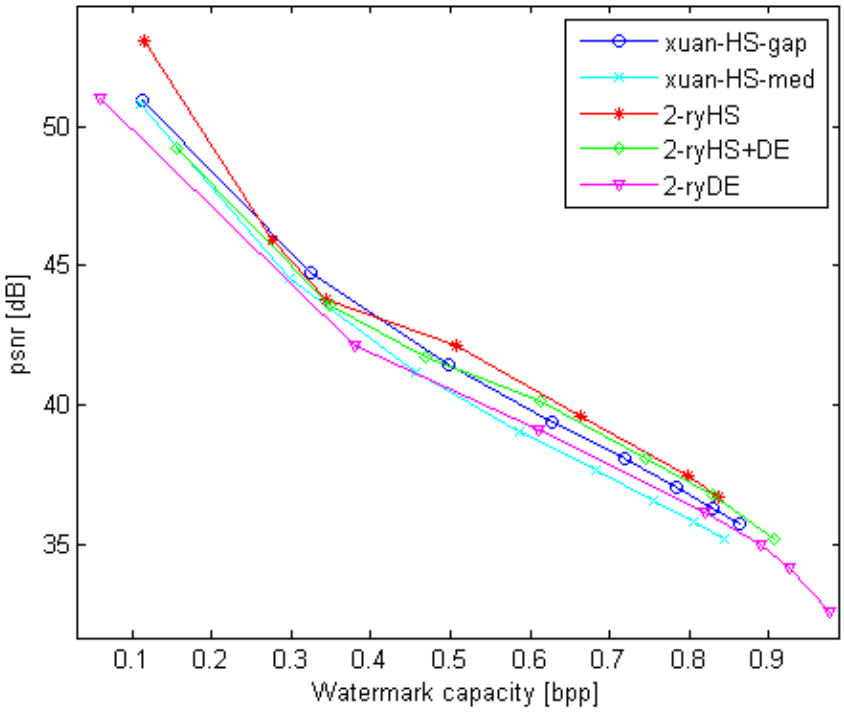

Figure 20: The embedding capacity versus image quality PSNR comparison curve for 512×512 Lena, $q = 2$

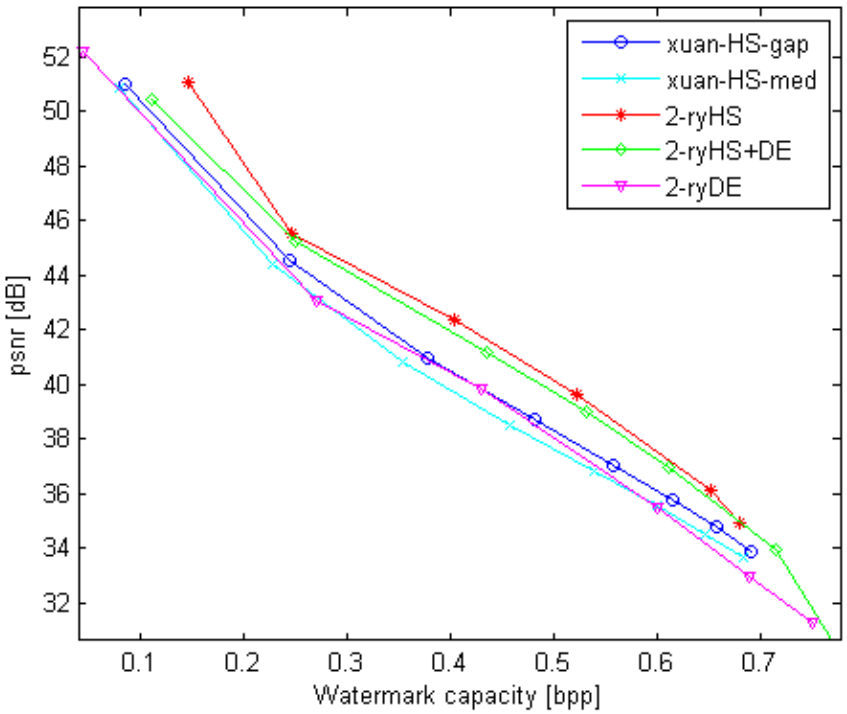

Figure 21: The embedding capacity versus image quality PSNR comparison curve for 512×512 Barbara, $q = 2$

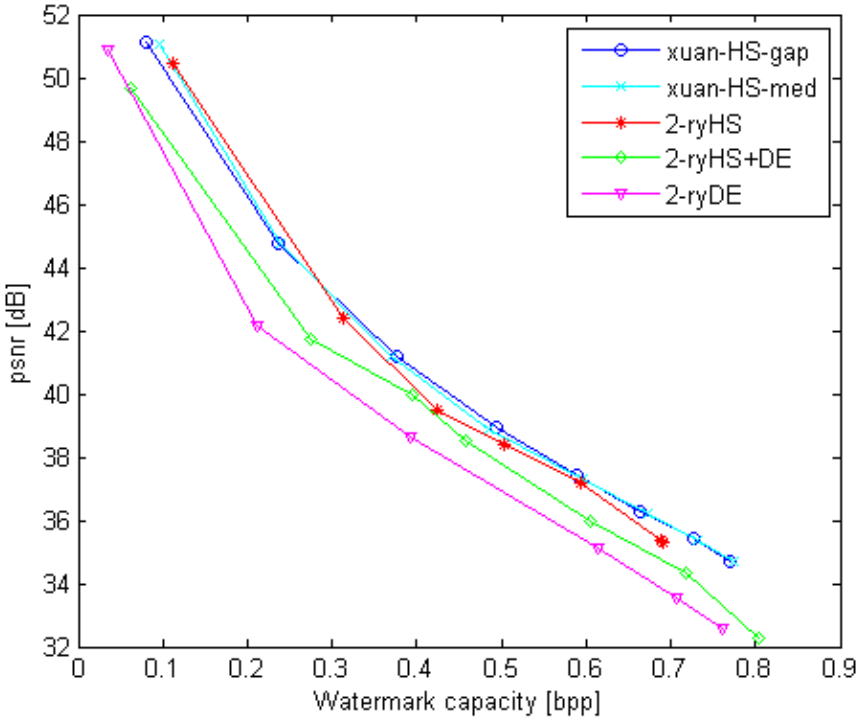

Figure 22: The embedding capacity versus image quality PSNR comparison curve for 512×512 Couple, $q = 2$

Moreover, Table 4 lists PSNR and payload size comparison of a number of data hiding methods [1, 4, 15, 19] with the proposed 2-aryHS+DE method for 512×512 grayscale Lena. Note that Coltuc in [4] developed the improvement embedding of the prediction error expansion scheme introduced by Thodi et. al. [15]. The proposed approach was realized for two implementations: DE and HS. The improved MED based on DE technique was determined by optimization with respect to the parameter α, which controls the amount of data to be embedded. However, it was stated in [4] that the loss in performance is completely insignificant if instead of varying α, a constant is considered.

The best results for Lena image were obtained when α equals to 0.12, thus, which corresponds to the best results as stated in [4]. It can be clearly seen that in average the proposed technique achieves 2 dB increase in quality compared to [1, 19] schemes around 3 dB compared to the original implementation of [15] and [4] MED scheme based on the DE, and shows similar behavior with [4] GAP scheme based on HS technique. Note that at smaller payloads, 2-aryHS+DE scheme is outperformed by [4] GAP technique with the average improvement of 0.8 dB, however, with the increase of payload, the proposed approach gains better quality. To further show the improvement of the proposed scheme, the 3-aryHS technique is compared with [4] HS based on GAP in Figure 23 for Lena image. At 32 dB our approach allows to embed 1.2 bpp, which is 0.22 bpp higher than the compared technique [4]. Moreover, the payload of 1.4 bpp can be obtained with the image quality of 31 dB.

Table 4: Comparison of embedded payload vs psnr (bpp, dB) of 512×512 Lena

Tian [1]		Hu [19]		Thodi [15]		Coltuc[4] DE, MED		Coltuc[4] HS, GAP		2-aryHS+DE	
bpp	**psnr**	bpp	**psnr**	bpp	**psnr**	bpp	**psnr**	bpp	**psnr**	bpp	**psnr**
0.1509	**44.20**	0.1029	**46.03**	0.15	**39.61**	0.15	**39.87**	0.15	**50.23**	0.1555	**49.19**
0.2429	**42.86**	0.2040	**44.46**	0.29	**38.61**	0.29	**38.89**	0.28	**46.43**	0.2896	**45.27**
0.3207	**41.55**	0.3051	**42.78**	0.35	**38.19**	0.35	**38.47**	0.33	**45**	0.3481	**43.6**
0.3856	**40.06**	0.4005	**40.31**	0.47	**37.34**	0.47	**37.64**	0.46	**42.5**	0.4697	**41.74**
0.4601	**37.66**	0.5035	**35.18**	0.6	**36.35**	0.61	**36.59**	0.6	**40.16**	0.6131	**40.13**
0.5398	**36.15**	0.6065	**34.76**	0.7	**35.47**	0.7	**35.84**	0.7	**38.2**	0.7005	**38.86**
0.6713	**34.8**	0.7057	**34.24**	0.73	**35.18**	0.73	**35.58**	0.73	**37.76**	0.737	**38.23**
0.8470	**32.54**	0.8010	**33.52**	0.88	**33.34**	0.88	**33.9**	0.89	**35.56**	0.8891	**35.59**
0.9919	**29.43**	0.9040	**32.24**	0.98	**31.42**	0.98	**32.41**	0.98	**32.37**	0.9855	**32.25**

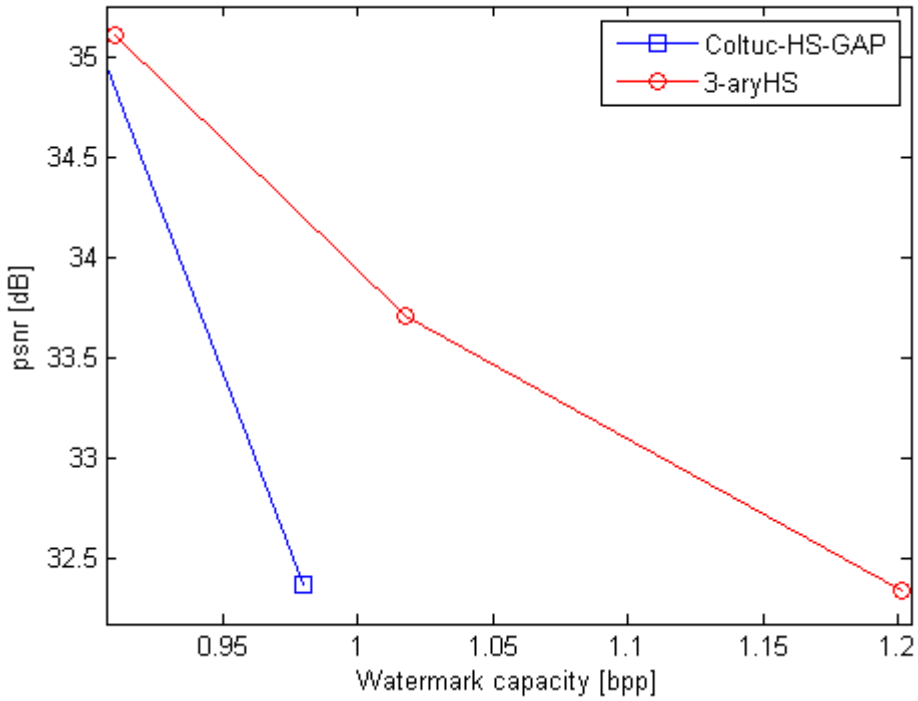

Figure 23: Watermarked 512×512 Lena comparison for 3-aryHS and Coltuc [4]

In order to determine the general behavior of the schemes the state-of-the-art technique in [4] is compared with the proposed method on a second set of 24 images of good quality. When running the algorithm in [4], the optimized version was computed and the best PSNR value for each value of the threshold was found. However, as it occurred some of the images cannot provide payload higher than 0.7 bpp. Therefore, when calculating the average we had to exclude them from consideration. Figure 24 shows the average payload versus image quality comparison of the proposed 2-aryDE+HS based on WSP and 2-aryDE based on GAP with the DE scheme based on MED, GAP [4]; and HS scheme based on MED prediction. Our advantage for the considered set of Kodak images in both of the DE schemes with MED and GAP prediction is evident. Moreover, the proposed

scheme can achieve a high payload of more than 0.7 bpp for each of the images.

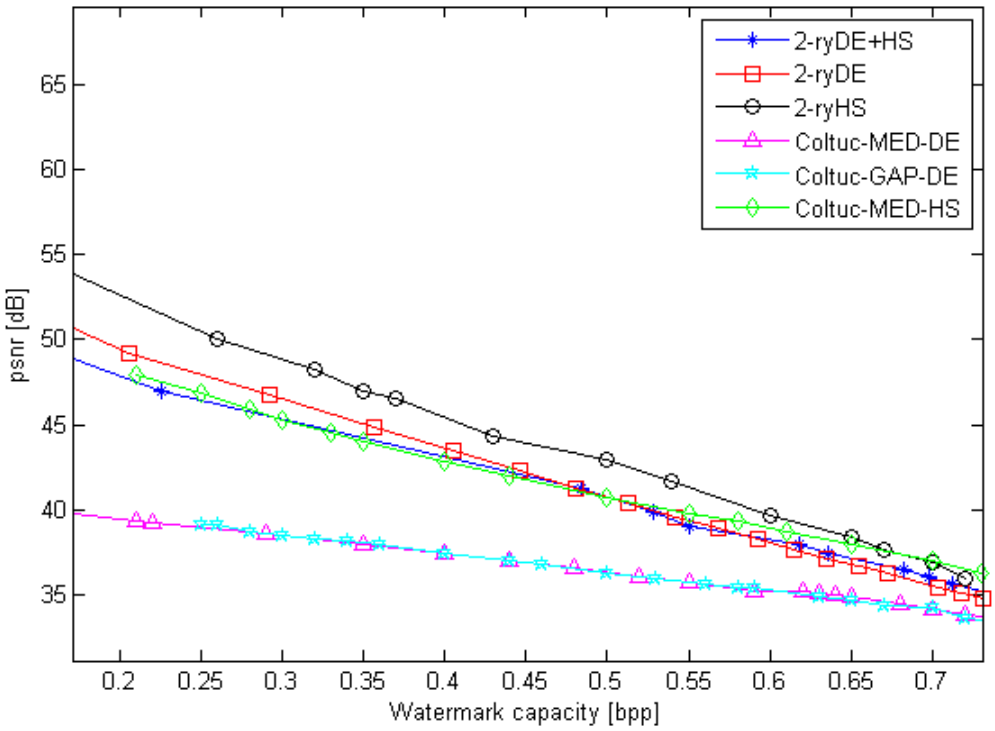

Figure 24: Average embedding capacity versus quality curves comparison of the proposed technique with [4] scheme for Kodak test images

After excluding the set of Kodak images, for which the DE and HS schemes in [4] do not work (namely, images: 5, 8, 13, 20, 24) for high payload the average improvement of our scheme compared to DE and HS schemes is around 0.76 dB. In order to evaluate the performance of the excluded images the 3-aryDE+HS scheme is considered and a set of experiments on the most ”difficult” images is performed, the statistical content of which do not allow to embed high payload in case of the scheme in [4]. Figures 25-27 consists of three payload versus quality plots obtained for images 5, 8 and 24 at high payloads, which show a very clear advantage of the proposed scheme in terms of the quality versus payload curves. Obviously, the proposed 3-aryDE+HS scheme is capable to embed of around 1 bpp with the same quality level.

All in all, after making experiments for two sets of images it can be stated that the scheme choice depends on the considered application. Basically if a small payload is required then 2-aryDE/HS/DE+HS techniques are suitable and show excellent performance. In case high payloads are to be achieved our 3-aryDE/HS/DE+HS schemes show a better performance.

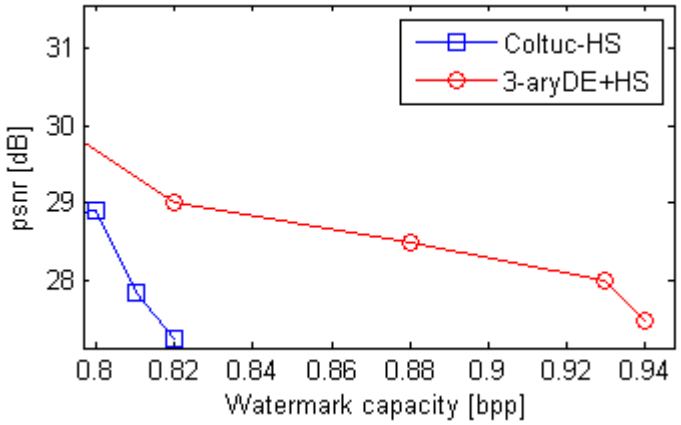

Figure 25: The embedding capacity versus image quality PSNR comparison curve for 5th Kodak image

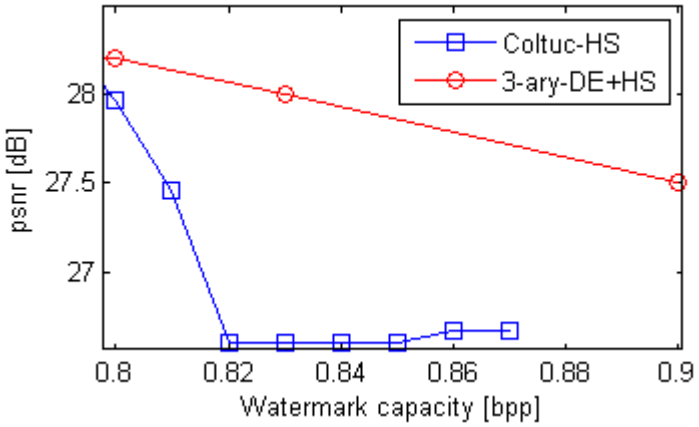

Figure 26: The embedding capacity versus image quality PSNR comparison curve for 8th image

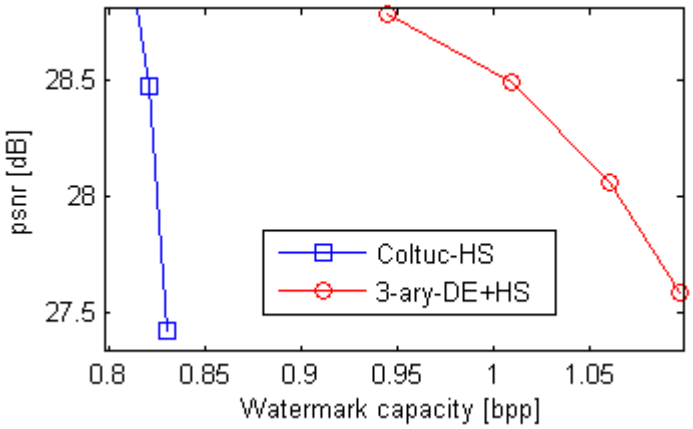

Figure 27: The embedding capacity versus image quality PSNR comparison curves for 24th image

The amount of payload can be enlarged by taking advantage of the local activity indicator. By bounding the statistical dispersion with thresholds $[T_{low}^{\mathrm{DE}}, T_{high}^{\mathrm{DE}}]$, $[T_{low}^{\mathrm{HS}}, T_{high}^{\mathrm{HS}}]$ it is possible to choose the to-be-embedded image frequencies along with the data hiding scheme by indicating valid thresholds for the desired embedding technique. Figure 28 presents three scenarios of binary embedding into 512 $\times$ 512 Man and Lena images, where the embeddable pixel positions are marked with the white color:

- 2-aryHS technique with $[T_{low}^{\mathrm{HS}}, T_{high}^{\mathrm{HS}}]$=[50,100], $Q = 3$ and, therefore, data hiding is done into high frequency components;
- 2-aryDE scheme with $[T_{low}^{\mathrm{DE}}, T_{high}^{\mathrm{DE}}]$=[0,10], and thus, secret message is hidden into low frequencies. Note that in that case there is no overhead information and the payload constitutes 0.82 bpp;
- 2-aryHS+DE technique with the thresholds $[T_{low}^{\mathrm{DE}}, T_{high}^{\mathrm{DE}}]$=[0,50], $[T_{low}^{\mathrm{HS}}, T_{high}^{\mathrm{HS}}]$=[50,100], $Q = 3$ with data hiding into low and high frequency components, respectively.

As it was mentioned earlier in order to reach high payload capacity, the secret data with elements from Galois field $GF(q)$, $q \geq 2$ is used. The following technique allows to embed more than one bit per pixel in a single run of an algorithm. However, our technique is also applicable to multiple embedding with excellent performance. In order to achieve high payload we utilize both DE and HS embedding scheme at the first layer of embedding with the following parameters: $[T_{low}^{\mathrm{DE}}, T_{high}^{\mathrm{DE}}]$=$[0, T]$, and $[T_{low}^{\mathrm{HS}}, T_{high}^{\mathrm{HS}}]$=$[0, 2T]$, where $T = [10, 20, 25, 35, 40, 50, 60], Q = 6$ and then only HS scheme at the second layer. The choice of the HS scheme in second layer embedding can be clarified by addressing the results visualized in Figure 19-22, where it showed high quality performance in comparison to other schemes. Table 5 demonstrates the multiple layer embedding possibility for Lena test image, whereas it also lists PSNR and payload size for various $q > 2$ technique scenarios that require one level of embedding.

Table 5: High capacity performance with multiple embedding or q-aryDE+HS scenarios in 512×512 Lena, $q > 2$

Scheme	Embedding Layer	Performance				
2-ryDE+HS	first out of two	psnr	35.62	33.45	32.56	32.08
		bpp	0.8829	0.9606	0.9788	0.9855
2-ryHS	second out of two	psnr	30.65	29.33	28.84	27.58
		bpp	1.2994	1.3944	1.4135	1.5432
		ssim	0.9472	0.9416	0.9399	0.9246
3-ryDE+HS	one	psnr	26.62	26.61	26.6	26.59
		bpp	1.5108	1.5113	1.5117	1.5121
4-ryDE+HS	one	psnr	24.64	24.59	24.5	24.4
		bpp	1.7936	1.8031	1.8116	1.8191

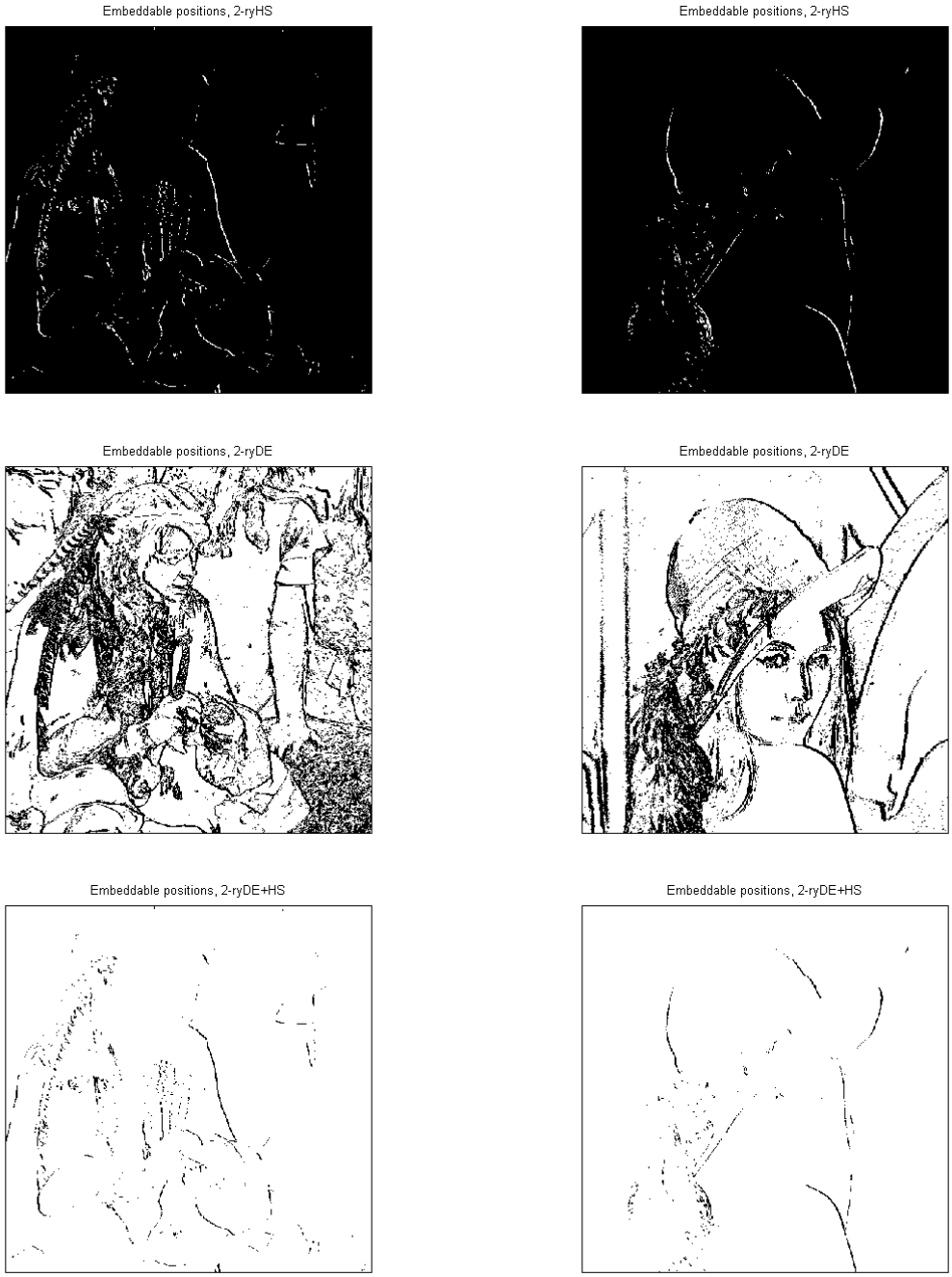

Figure 28: The embeddable positions (white color) of 512×512 Man and Lena for 2-aryHS (first row), 2-aryDE (second row) and 2-aryHS+DE (third row) schemes

Note that the proposed scheme can be applied to test images in various color spaces. Here we perform 2-aryDE+HS data hiding procedure into 24-bit Lena image in RGB color space with the following parameters: $[T_{low}^{\mathrm{DE}}, T_{high}^{\mathrm{DE}}]$=[0,50], $[T_{low}^{\mathrm{HS}}, T_{high}^{\mathrm{HS}}]$=[0,150], $Q = 3$. In this case, we managed to embed 0.9372 bpp into Lena at the quality of 30.98 dB. The watermarked image can be visualized in Figure 29.

Figure 29: Watermarked 512×512 Lena for 2-aryHS+DE

5.4 The performance of the proposed DH scheme in the frequency domain

The performance of the proposed data hiding scheme in the frequency domain is measured by examining its capacity, distortion and its effect on the file size. The result of our experiment on the second set of images can be visualized in Figure 30, where we presented the average performance of all the images at various JPEG compression quality levels $Q_f = [60, 70, 80, 90]$. The result of our experiment on 512 $\times$ 512 Lena and Mandrill are summarized in Table 6, where we presented the achieved performance at a JPEG compression quality level $Q_f = 75$. Here, we omit the prediction operation to avoid pixel dependency and increase robustness. The possible compression ratio at the defined quality level of Lena and Mandrill images without watermarking corresponds to 8.02 and 3.26, respectively. Note that the obtained results of embedding capacity and quality of the watermarked image in JPEG format are higher than those achieved in a number of data hiding algorithms, such as [32] and [33]. In fact, in [32] the algorithm enables embedding of 1040 bits in Lena and Mandrill at the quality of 40.87 and 43.28 dB, respectively. All in all, as can be seen in Table 6, the proposed approach show quite a high performance. Note that in case $h = 1, Q = 3$, which correspond the last lines in the table for each of the images, we performed the search of the embeddable AC. The payload is obviously lower, however, the compression ratio is preserved to be high. A similar behavior can be visualized by hiding the secret message, when $h = 1$ compared to $h = 0$. In summary, it can be concluded that the proposed data hiding method operates efficiently both in the

spatial and frequency domains.

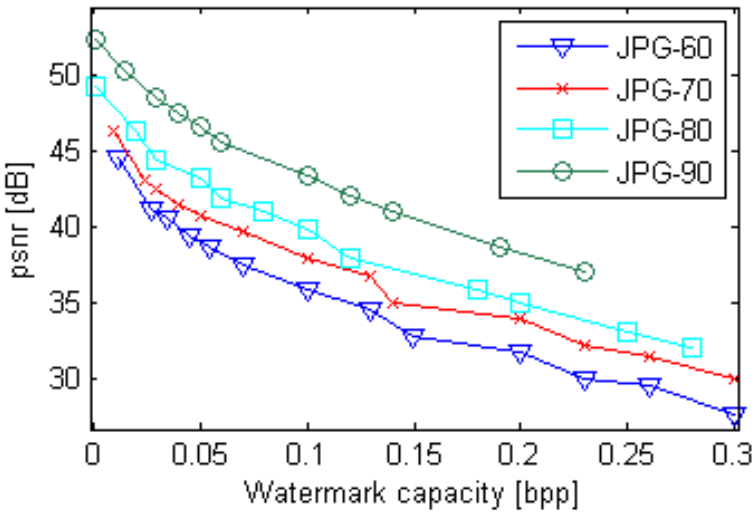

Figure 30: Average PSNR versus payload curves for the set of Kodak test images in JPEG format with different quality factors 60, 70, 80 and 90

Table 6: Performance of Lena and Mandrill images in JPEG format

Image	Parameters			Payload	PSNR	Ratio
	h	Q	AC_k	(bits)	(vs JPEG image)	
Lena	0	1	[2 : 6]	7059	44.50	7.68
	0	1	[2 : 25]	64910	33.44	5.56
	0	3	[2 : 25]	82250	30.53	5.43
	1	1	[2 : 25]	12933	40.83	7.5
	1	3	[2 : 25]	19684	34.96	7.28
	1	3	[1,2,11,16,22,29,48,53,61]	2567	37.59	7.91
Mandrill	0	1	[2 : 6]	2566	43.93	3.21
	0	3	[2 : 25]	65296	26.62	2.84
	0	1	[2 : 25]	32409	43.93	3.21
	1	1	[2 : 25]	22801	35.38	3.1
	1	3	[2 : 25]	39265	29.23	3
	1	3	[15,16,22,26:29,35,36,37,41]	10846	33.93	3.22

Conclusion

In conclusion, let us summarize the most important results of the performed studies.

1. An extensive literature review was conducted that set the base for understanding the main concepts of the state-of-the art watermarking techniques.

The topic of data hiding has gained a lot of attention by the researchers during the last decade and is still very popular nowadays, which is proved by the numerous scientific papers that are published every year. In order to contribute to the given research field a clear understanding of the main concepts was required, and was obtained by classifying the data hiding schemes based on various concepts: reversibility property, the technique of data embedding, and domain of operation. After narrowing the list to the papers-of-interest, the latter, among which are DE-based schemes [1, 4] and HS-based techniques [5, 6], were investigated in detail.

2. A thorough analysis of the reversible DE and HS techniques allowed to outline the main limitations and constraints of the schemes in terms of auxiliary data, computational efficiency, flexibility and capacity.

Therefore, the data hiding scheme based on DE and HS embeddings was proposed that aimed at improving the following concepts:

- **auxiliary data**: the thresholds $T_{low}^{\mathrm{DE}^*}$, $T_{high}^{\mathrm{DE}^*}$ and $T_{low}^{\mathrm{HS}^*}$, $T_{high}^{\mathrm{HS}^*}$ for DE and HS embeddings that allow data hiding with no overhead information were found, i.e. location map free data embedding was achieved.

- **computational efficiency**: a new weighted simplified predictor, which can achieve an improvement in terms of computational costs, which is shown in Table 3, was developed.

- **flexibility**: local activity indicator as a measure of some statistical dispersion that allowed to choose the target embedding image frequencies was introduced.

- **capacity**: the secret message with the elements from Galois field was used to achieve the capacity of more than 1 bit per pixel in a single run of an algorithm.

3. The scheme in spatial domain was compared with a number of data-hiding methods [1], [4]-[6], [15, 19], where the proposed technique showed a clear advantage in terms of payload versus quality performance.

Particularly, when comparing with the state-of-the-art scheme in [4], which showed an excellent performance especially at the high payloads of around 1 bpp, the following important conclusion was derived: the proposed scheme choice depends on the considered application. Basically if a small payload is required then 2-aryDE/HS/DE+HS techniques are suitable and show excellent performance. In case high payloads are to be achieved our 3-aryDE/HS/DE+HS schemes show a better performance.

4. The generalized approach with combined DE and HS embeddings was extended to JPEG format images, which represents the common compression standard for transmission and storage of digital images.

The performance of the scheme in the frequency domain was measured by examining capacity, distortion and the effect on the file size. The introduced technique outperformed a number of data hiding algorithms developed in [32, 33].

5. The scheme can achieve high performance on conducting multiple layer embeddings and secret message hiding in color test images, which was revealed in Table 5 and in Figure 29.

Thus, the proposed watermarking approach holds the advantages of the location map free data embedding, is invariant to the choice of predictor, enables high payload capacity due to the utilization of secret data with elements from Galois field and can be easily extended to JPEG format images. In the future, we plan to investigate the use of data hiding techniques in image error concealment schemes.

References

[1] J. Tian, ”Reversible Data Embedding Using a difference expansion”, *IEEE Trans. on Circuits and Systems for Video technology*, 2003, 13(8), pp. 890-896.

[2] T. Efimushkina, and K. Egiazarian, ”High-Capacity Reversible q-ary Data Hiding with Location Map-Free Capability”, *Proc. of International Conference on Imaging for Crime Detection and Prevention*, London, UK, Nov. 3-4, 2011, pp. 39-48.

[3] T. Efimushkina, and K. Egiazarian, ”Reversible q-ary Watermarking with Controllable Prediction Error and Location Map-Free Capability”, *Proc. of SPIE 8303, Media Watermarking, Security, and Forensics*, Burlingame, California, Jan. 22, 2012, vol. 830308.

[4] D. Coltuc, ”Improved embedding for prediction-based reversible watermarking”, *IEEE Trans. on Information Forensics and Security*, 2011, 6(3), pp. 873-882.

[5] G. Xuan, Q. Yao, Q. C. Yang, J. Gao, P. Chai, Y. Shi, and Z. Ni, ”Lossless data hiding using histogram shifting method based on integer wavelets ”, *Proc. of 5th International Workshop on Digital Watermarking*, Korea, Nov. 2006, vol. 4283, pp. 323-332.

[6] Z. Ni, Y. Q. Shi, N. Ansari, and W. Su, ”Reversible data hiding”, *IEEE Transactions on Circuits and Systems For Video Technology*, March 2006, 16(3), pp. 354-362.

[7] C. Honsinger, P. Jones, M. Rabbani, and J. Stoffel, ”Lossless recovery of an original image containing embedded data”, *U. S. Patent 6 278 791*, 2001.

[8] B. Macq, ”Lossless multiresolution transform for image authenticating watermarking”, *Proc. of EUSIPCO*, Tampere, Finland, Sept. 2000, pp. 533-536.

[9] J. Fridrich, M. Goljan, and R. Du, ”Lossless data embedding - new paradigm in digital watermarking”, *EURASIP Journal on Applied Signal Processing*, 2002, pp. 185-196.

[10] M. U. Celik, G. Sharma, A. M. Tekalp, and E. Saber, ”Lossless generalized-LSB data embedding”, *IEEE Transactions on Image Processing*, Feb. 2005, 14(2), pp. 253-266.

[11] M.U. Celik, G. Sharma, A.M. Tekalp, ”Lossless watermarking for image authentication: a new framework and an implementation”, *IEEE Trans. Image Processing*, 2006, 15 (4), pp. 1042-1049.

[12] A. Alattar, “Reversible watermarking using difference expansion of triplets”, *IEEE International Conference on Image Processing*, Catalonia, Spain, Sept. 2003, vol. 1, pp. 501-504.

[13] A. Alattar, “Reversible watermarking using difference expansion of quads”, *Proc. of IEEE International Conference on Acoustics, Speech and Signal Processing*, Montreal, Canada, May 2004, vol. 3, pp. 377-380.

[14] D. Thodi and J. Rodriguez, ”Prediction-error based reversible watermarking”, *Proc. of International Conference on Image Processing*, Genova, Oct. 2004, vol. 3, pp. 1549-1552.

[15] D. Thodi and J. Rodriguez, ”Expansion embedding techniques for reversible watermarking”, *IEEE Transactions on Image Processing*, 2007, 16(3), pp. 721-730.

[16] H. W. Tseng, and C. P. Hsieh, ”Prediction-based reversible data hiding”, *Journal of Information Science*, 2009, vol. 179, pp. 2460-2469.

[17] H. C. Wu, C. C. Lee, C. S. Tsai, Y. P. Chu, and H. R. Chen, ”A high capacity reversible data hiding scheme with edge prediction and difference expansion”, *IEEE Trans. on Information Forensics and Security*, 2007, vol. 2, pp. 311-319.

[18] X. Wang, C. Shao, X. Xu, and X. Niu, ”Reversible data-hiding scheme for 2-D vector maps based on difference expansion”, *Journal of Systems and Software*, 2009, vol. 82, pp. 1966-1973.

[19] Y. Hu, H.-K. Lee, K. Che, and J. Li, ”DE-based reversible data hiding using two embedding directions”, *IEEE Transactions on Multimedia*, 2008, vol. 8, pp. 1500-1512.

[20] L. Luo, Z. Chen, M. Chen, X. Zeng, and Z. Xiong,”Reversible image watermarking using interpolation technique”, *IEEE Trans. on Information Forensics and Security*, 2010, 5(1), pp. 187-193.

[21] B. Yang, M. Schmucker, W. Funk, C. Busch, and S. Sun, ”Integer DCT-based reversible watermarking for images using companding technique”, *Proc. of SPIE, Security and Watermarking of Multimedia Content, Electronic Imaging*, San Jose, California, USA, Jan. 18-22, 2004, vol. 5306, pp. 405-415.

[22] J. Hwang, J. Kim, and J. Choi, ”A reversible watermarking based on histogram shifting”, *Proc. of International Workshop on Digital Watermarking*, Jeju Island, Korea, Nov. 8-10, 2006, pp. 348-361.

[23] C. C. Chang C. C. Lin, W. L. Tai, ”Multilevel reversible data hiding based on histogram modification of difference images”, *Pattern Recognition*, 2008, vol. 41, pp. 3582-3591.

[24] P. Tsai, Y. C. Hu, and H. L. Yeh, ”Reversible image hiding scheme using predictive coding and histogram shifting”, *Signal Processing*, 2009, 89(6), pp. 1129-1143.

[25] K. Kim, M. Lee, H.-Y. Lee, and H.-K. Lee, "Reversible data hiding exploiting spatial correlation between sub-sampled images", *Pattern Recognition*, 2009, 42(11), pp. 3083-3096.

[26] C. Chen, Z. Chen, X. Zeng, and Z. Xiong, "Reversible data hiding using additive prediction-error expansion", *Proc. of the 11th ACM Workshop on Multimedia and Security*, Princeton, NJ, 2009, pp. 16-21.

[27] W. Hong, T. Chen, and C. Shiu, "Reversible data hiding for high quality images using modification of prediction errors", *The Journal of Systems and Software*, 2009, 82(11), pp. 1833-1842.

[28] M. Fallahpour, and H. Sedaaghi, "High capacity lossless data hiding based on histogram modification", *IECIE Electronic Express*, 2007, 4(7), pp. 205-210.

[29] M. Fallahpour, "Reversible image data hiding based on gradient adjusted prediction", *IECIE Electronic Express*, 2008, vol. 5, pp. 870-876.

[30] C. Chang, T. Chen, and L. Chung, "A steganographic method based upon JPEG and quantization table modification", *Information Sciences*, 2002, vol. 141, pp. 123-138.

[31] J. Fridrich, M. Goljan, and R. Du, "Lossless data embedding for all image formats", *Proc. of SPIE, Electronic Imaging, Security and Watermarking of Multimedia Contents IV*, San Jose, Jan. 2002, vol. 4675, pp. 572-583.

[32] G. Xuan, Y.-Q. Shi, and Z. Ni, "Reversible data hiding for JPEG images based on histogram pairs", *Proc. of Image Analysis and recognition, 4th International Conference*, Montreal, Canada, Aug. 22-24, 2007, vol. 4633, pp. 715-727.

[33] H. Sakai, M. Kuribayashi, and M. Morii, "Adaptive reversible data hiding for JPEG images", *Proc. of International Symposium on Information Theory and its Applications*, Auckland, New Zealand, Dec. 7-10, 2008, pp. 870-875.

[34] H. Jin, M. Fijiyoshi, and H. Kiya, "Lossless data hiding in the spatial domain for high quality images", *IEICE Transactions on Fundamentals of Electronics, Communications and Computer Sciences*, 2007, pp. 771-777.

[35] A. Aznaveh, F. Torkamani-Azar, A. Mansouri, and F. Kurugollu, "Reversible watermarking using statistical information", *EURASIP on Advances in Signal Process*, 2010, vol. 2.

[36] D. Coltuc, and J.-M. Chassery, "Very fast watermarking by reversible contrast mapping", *IEEE Signal Processing Letters*, 2007, 14(4), pp. 255-258.

[37] J. Kornblum, "Using JPEG quantization tables to identify imagery processed by software", *Proc. of the Digital Forensic Workshop*, Aug. 2008, pp. 21-25.

[38] A. Wong, and J. Orchard"A nonlocal means approach to exemplar-based inpainting", *Proc. of IEEE International Conference on Image Processing*, San Diego, Dec. 2008, pp. 2600-2603.

[39] A. Buades, B. Coll, and J. M. Morel"A non-local algorithm for image denoising", *Proc. of the International Conference on Computer Vision and Pattern Recognition*, San Diego, CA, USA, June 20-26, 2005, pp. 60-65.

[40] UWaterloo image database [Online], links.uwaterloo.ca/Repository.html.

[41] Kodak image database [Online], http://www.r0k.us/graphics/kodak/.

[42] S. Voloshynovskiy, S. Pereira, A. Herrigel, N. Baumgartner, and T. Pun, "Generalized watermarking attack based on watermark estimation and perceptual remodulation", *SPIE Symposium on Electronic Imaging*, 2010, vol. 3971.

[43] Z. Wang, A. Bovik, H. Sheikh, and E. Simoncelli, "Image quality assessment: From error visibility to structural similarity", *IEEE Trans. on Image Processing*, 2004, 13(4), pp. 600-612.